Mineralium Deposita (2023) 58:569–591
https://doi.org/10.1007/s00126-022-01147-7

ARTICLE

Genesis of the exotic chrysocolla — "copper pitch/wad" — atacamite/brochantite ore at the Exótica (Mina Sur) deposit, Chuquicamata, Chile

Bernhard Dold[1,2] · **Marie-Caroline Pinget**[1] · **Lluís Fontboté**[1]

Received: 10 November 2020 / Accepted: 7 October 2022 / Published online: 9 November 2022

Abstract

Detailed mineralogical and textural studies, combined with sequential X-ray diffraction and geochemical modeling, helped to solve the "copper pitch/wad" enigma in the Exótica deposit located downstream of the Chuquicamata porphyry copper deposit. Copper pitch and copper wad are essentially chrysocolla with co-precipitated Mn oxides, mainly birnessite, as well as pseudo-amorphous Mn oxide/oxyhydroxides. Linking the mineralogical, geochemical, and textural evidences with the geological, tectonic, and climatic evolution of the Chuquicamata–Calama area, a four-step genetic model for the evolution of the Exótica deposit is presented: (A) formation of a mature supergene enrichment profile at Chuquicamata (~30–25 Ma to ~15 Ma) during an erosion-dominated regime (~900 m of erosion) which was accompanied by acidic (pH ~2–4) Cu-Mn-Si-dominated rock drainage (ARD) with fluid flow southwards through the Exótica valley towards the Calama Basin, resulting in a strongly kaolinized and chrysocolla/copper wad-impregnated bedrock of the Exótica deposit; (B) deposition of the Fortuna gravels in the Exótica valley (starting ~19 Ma) intercepted the Cu-Mn-Si-dominated ARD, triggering the main chrysocolla, copper pitch/wad mineralization as syn-sedimentary mineralization by chiefly surficial flow in strongly altered gravels; (C) tectonic freezing and onset of hyper-aridity (~15–11 Ma) exposed the enriched chalcocite blanket of Chuquicamata to oxidation, resulting in acidic (pH ~ 2–4) and Cu-Si-dominated solutions with less Mn. These solutions percolated in a slightly more reducing groundwater flow path and mineralized relatively unaltered gravels with pure chrysocolla; and (D) ingression of confined chloride-rich groundwater in the upper oxidation zone of Chuquicamata, most likely between 6 and 3 Ma, is responsible for the atacamite/brochantite mineralization (pH ~ 5.5–7) of mainly unaltered gravels in the northern and central part of the Exótica deposit.

Keywords Birnessite · Solubility · Acid rock drainage · Exotic mineralization · Saline groundwater · Supergene

Introduction

Supergene processes and exotic deposits

Porphyry copper deposits, when exposed to oxidizing conditions by uplift and erosion (atmospheric oxygen and water with high partial pressure of oxygen), develop characteristic oxidation profiles (Brimhall et al. 1985; Ague and Brimhall 1989; Sillitoe 2005; Pinget 2016). In the oxidation zone, the oxidation of hypogene sulfide minerals results in acid rock drainage (ARD) and formation of secondary mineral assemblages. The development of the oxidation zone depends principally on the hypogene sulfide mineralogy, on the neutralization potential of the gangue minerals, and on the existence of an unsaturated zone; this last parameter is controlled by tectonics, climate, erosion, and incision of the hydrographic network (Brimhall et al. 1985; Alpers and Brimhall 1989; Sillitoe 2005; Hartley and Rice 2005).

Copper transported in acid solutions in the oxidation zone can precipitate as "copper oxides," a term that, in this context, refers to non-sulfide copper minerals and includes oxides, hydroxides, silicates, sulfates, phosphates, and carbonates (Brimhall et al. 1985; Padilla Garza et al. 2001). The precipitation of copper minerals in the oxidation zone is largely controlled by pH and activities of the solutes

Editorial handling: F. Tornos

✉ Bernhard Dold
bdold@sumirco.com

[1] Department of Earth Sciences, University of Geneva, Geneva 1205, Switzerland

[2] Pontifical Catholic University of Peru (PUCP), San Miguel, Lima 15088, Peru

(Anderson 1982; Sillitoe 2005). From acidic to neutral conditions, the following sequence is typically observed: chalcanthite, antlerite, brochantite, and tenorite. Chrysocolla can precipitate instead of brochantite in the presence of silica, malachite, and azurite in the presence of carbonate and atacamite in the presence of chloride.

Copper mobilized downwards by ARD below the water table may reprecipitate as covellite and chalcocite–digenite–djurleite in a reducing environment. This enrichment ("chalcocite blanket") is recognized in numerous porphyry deposits, including at the Chuquicamata porphyry copper deposit (Ossandón et al. 2001; Pinget 2016).

If the copper-bearing solutions derived from ARD migrate laterally under mainly oxic conditions, they may form an "exotic" copper deposit. In this case, the main precipitation mechanism is the pH increase by water–rock interaction with the bedrock. Exotic deposits contain typically chrysocolla and copper pitch/wad and in some cases atacamite (Newberg 1967; Münchmeyer 1996; Fernández-Mort et al. 2018; Riquelme et al. 2018). In southern Peru and northern Chile, conditions favorable for the formation of exotic deposits prevailed at least between late Oligocene and middle Miocene (Münchmeyer 1996; Sillitoe 2005; Fernández-Mort et al. 2018). Exotic deposits in Chile include Damiana in Cerro Indio Muerto, Huinquintipa in the Collahuasi porphyry copper deposit, El Tesoro in the Sierra Gorda district (Münchmeyer 1996; Fernández-Mort et al. 2018), and Centinela district (Riquelme et al. 2018; Sanchez et al. 2018). Exotic deposits have been described also in North America, for example, from the Ray porphyry copper deposit (Sillitoe 2005) and in other parts of the world like in the Oyu Tolgoi porphyry Cu-Au(-Mo) deposit, Mongolia (Perelló et al. 2001), the Bayugo porphyry copper gold deposit, Philippines (Braxton and Mathur 2011), and in the Chagai Cu-porphyry belt in Pakistan (Perelló et al. 2008).

The Exótica deposit is located south of Chuquicamata (Figs. 1 and 2). Mineral resource estimates are 310 Mt at 1.17% Cu (Ossandón et al. 2001). The Exótica deposit is also known as Mina Sur and is the product of laterally migrating acid rock drainage from the sulfide oxidation zone of the Chuquicamata porphyry copper deposit (Mortimer et al. 1978; Münchmeyer 1996; Ossandón et al. 2001; Pinget 2016). The present study on the Exótica deposit focuses on the mineralogical characterization and poorly understood formation mechanisms of copper pitch and copper wad and presents a four-step model of the formation of the deposit. In addition of optical microscopy, SEM–EDS, and bulk rock geochemistry, ICP-MS and XRD analysis of sequential extractions proved to be particular useful to characterize these poorly crystallized phases. Geochemical modeling with PHREEQC (Parkhurst and Appelo 2013) was used to propose the geochemical boundary conditions of

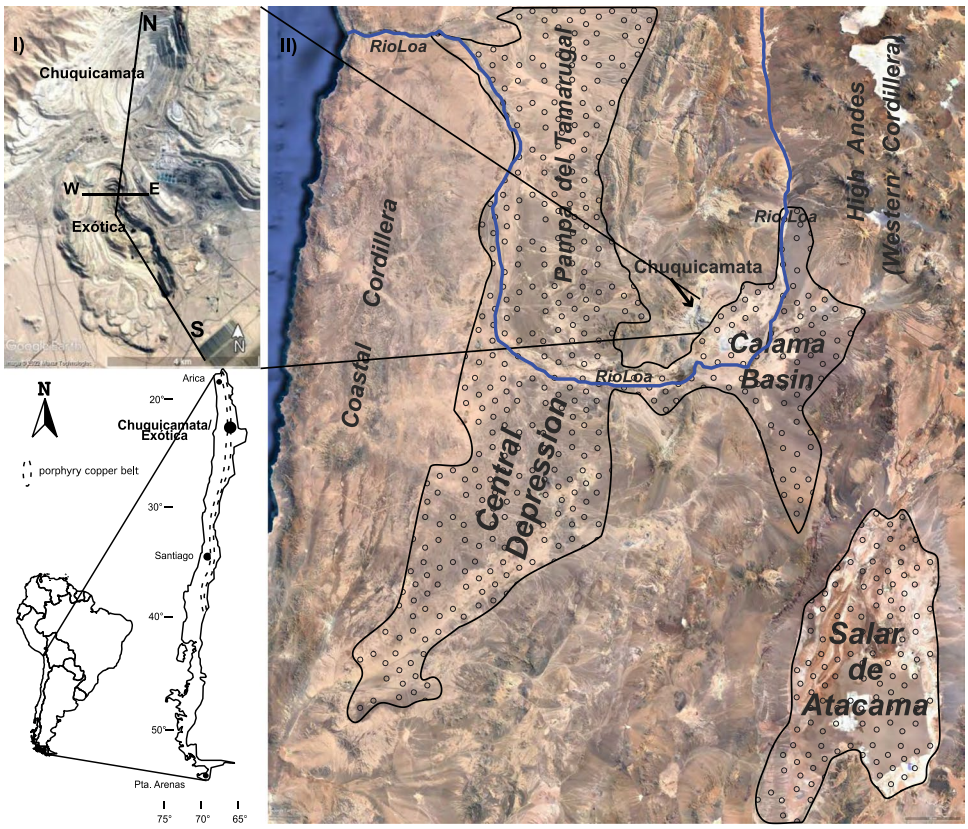

Fig. 1 Location and Google Earth® view of the Chuquicamata/Exótica complex in Northern Chile with the principal sedimentary basins (circle texture) in the region and the Rio Loa. In **I**, the location of the schematic vertical N-S and W-E cross-sections of Fig. 12 are given

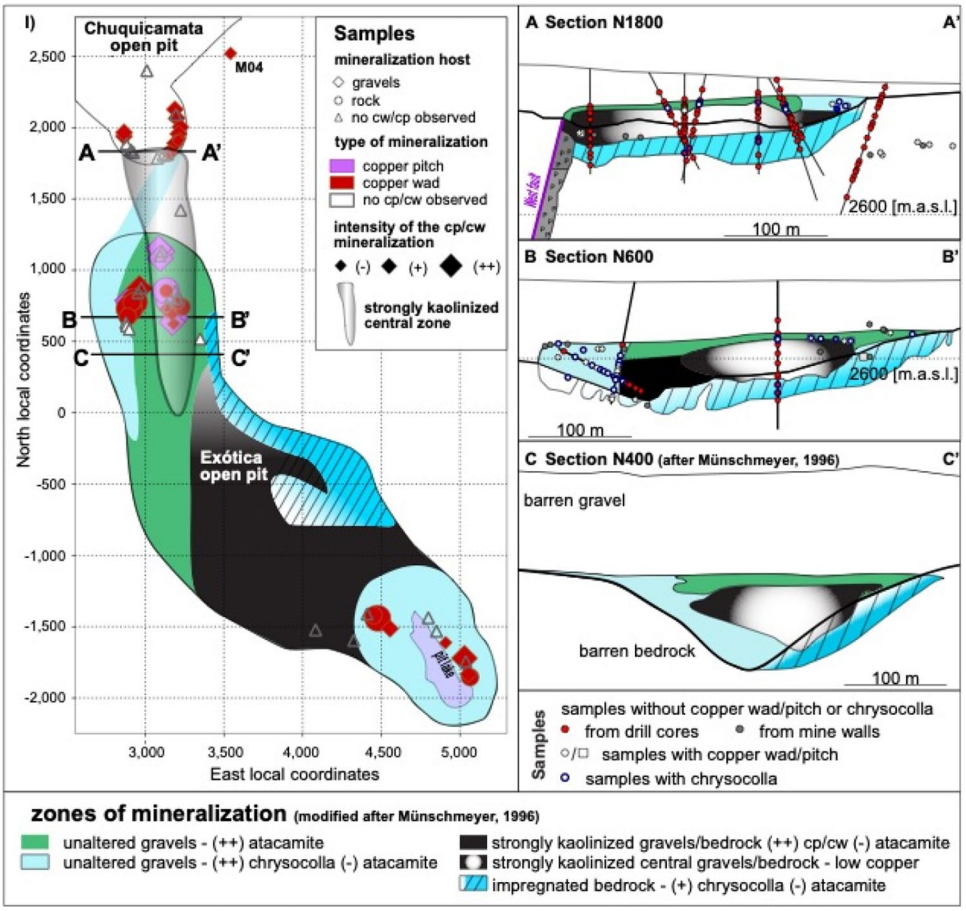

Fig. 2 I Overview of the sample locations in the Exótica deposit, mainly in the Exótica (Mina Sur) pit and subordinate in the southern part of the Chuquicamata pit used for this study. The mineral distribution was completed in the southern part of the Exótica pit after Münchmeyer (1996), which was exploited before the present study. **A**–**C** represent cross-sections along the N-S flow path of the mineralizing solutions. For detailed sample locations see Fig. ESM A.1

the formation of the exotic mineral assemblage. The resulting genetic model is set in context with the tectonic and climatic evolution of the Atacama Desert and the supergene enrichment at Chuquicamata since the Oligocene. The present work is complemented by studies on the supergene profile at the Chuquicamata main mineralization where was sourced the Cu-Mn-rich ARD that formed the Exótica deposit (Pinget 2016; Pinget et al. 2015). Present-day copper gel-like precipitates in the Exótica open pit are morphological similar to macroscopic ore textures of the Exótica deposit and were studied by Lambiel et al. (2022).

Geological setting of the Exótica deposit

The Exótica deposit extends, with a negative slope of 3 to 7°, for more than 7 km south of the Chuquicamata porphyry copper deposit (Figs. 1, 2, and 12). It was mined between 1957 and 2015. Supergene solutions from the oxidation zone of the Chuquicamata deposit interacted with underlying bedrock and the Miocene Fortuna and Exótica gravels forming the Exótica mineralization due to water–rock interactions (Mortimer et al. 1978; Newberg 1967; Münchmeyer 1996; Pinget 2016). The Fortuna gravels cover most of the mine site and are slope talus deposits with angular to sub-rounded clasts up to 2 m in diameter. They derived mainly from the adjacent Fortuna granodiorite and its deposition started therefore before the ~35 km sinistral strike-slip displacement along the West fault, that took place after 19 Ma according Lindslay (1997). The Exótica gravels occur in the northern part of the deposit, partly underlying the Fortuna gravels and partly interfingering with them. They consist of mud flow deposits including coarser intercalations of sand and small angular clasts up to 5 cm in diameter. Based on tectonic considerations and on an ash-tuff bed dated at 8.4 ± 0.4 Ma (K/Ar) interbedded in the upper part of the Fortuna gravels, Mortimer et al. (1978) proposed a mid-Miocene age for both gravel units, i.e., contemporaneous to the El Loa Group in the Calama Basin (May et al. 1999, 2005). Oxidized and mineralized Chuquicamata granodiorite porphyry clasts occur near the base of the gravel units. Newberg (1967) indicated that gravel deposition started when the porphyry copper deposit was already exposed to oxidation and erosion. Newberg (1967) also reported sedimentary reworking of clasts with broken rims of exotic mineralization in the northern part of the Exótica deposit suggesting that the gravel deposition was contemporaneous with the main exotic mineralization process.

As discussed in more detail below, the supergene enrichment at Chuquicamata is estimated to start at ~30–25 Ma (Mortimer et al. 1978) and, on the basis of K–Ar dating of supergene alunite (K. Wemmer, written communication, 2018), lasted at least until 11 Ma. Taking in account that, as explained above, the Fortuna gravels -main host of the Exótica deposit- have a maximum age of around 19 Ma, the in situ 18.4 ± 1 Ma U–Pb LA-ICP-MS dating of pseudomalachite associated to the chrysocolla/copper pitch mineralization (Kahou et al. 2021) can be considered as close to a maximum age of the start of the formation of the Exótica deposit.

Sedimentary evolution and hydrogeology of the Calama basin

The Calama basin-fill started in the Eocene with deposition of alluvial braidplain deposits (Calama Formation) on the basement of extensively faulted and brecciated Paleozoic metamorphic rocks and a Permian to Carboniferous igneous complex (Ossandón et al. 2001). From 22 to 10 Ma, ephemeral fluvial sediments were deposited along the Calama basin flanks (Lasana Formation), with a transition to playa sandflats and mudflat deposits (Jalquinche Formation) towards the endorheic basin center (May et al. 2005). The Pampa del Tamarugal and Calama basin areas were connected around 6 Ma. Regional palustrine carbonate sedimentation occurred in the Calama basin center recognized as the Opache Formation (May et al. 2005; Jordan et al. 2015). During the formation of the Opache Formation (6–3 Ma), a wetter period with high water levels in the endorheic Calama basin is assumed (May et al. 2005; Sáez et al. 2012). After 3 Ma, the Loa river reached its entrenchment through Miocene and Pliocene strata and connected through the Pampa Tamarugal to the Pacific (May et al. 2005).

The Calama and Opache Formation are aquifers in the system, while the Jalquinche Formation acts as an aquitard in-between. The lower confined aquifer is mainly related to the Calama Formation, while the upper phreatic aquifer is roughly located in the Opache Formation. However, due to the local heterogeneity of the sedimentary systems in the large Calama basin, connections between the two aquifers are assumed (Jordan et al. 2015). The head of the lower confined aquifer can locally exceed the head of the upper aquifer, for example, in the western part of the Calama basin, in the area east of Chuquicamata (Jordan et al. 2015). The lower aquifer has high salinity, as observed in the southernmost part of the Exótica open pit (Lambiel et al. 2022) and below the Talabre tailings impoundment in an artesian well (Smuda et al. 2014).

The study area was subjected to uplift since ~50 Ma with a period of reduced uplift rate when the Central Andes entered a tectonic "freezing" period between ~15 and 11–10 Ma (Armijo et al. 2015). The climate changed to arid conditions at ~30 Ma and at ~15 Ma towards a hyper-arid climate (Armijo et al. 2015). Several authors propose an uplift of the area of 1200–900 m in the last 11 Ma (May et al. 2005; Rech et al. 2006; Sáez et al. 2012; Armijo et al. 2015; Jordan et al. 2015). The dewatering of the Calama basin through the Rio Loa entrenchment after 3 Ma together with the uplift and hyper-aridity resulted in lowering of groundwater levels in the Calama basin to the today's observed levels.

Chrysocolla, copper pitch and wad, and atacamite

The principal copper-bearing phases in the Exótica deposit are chrysocolla, copper pitch/wad, and atacamite (Münchmeyer 1996; Pinget 2016). While atacamite ($Cu_2(OH)_3Cl$) is a well-defined crystalline mineral, chrysocolla ($(Cu_{2-x}Al_x(H_{2-x}Si_2O_5)(OH)_4 \bullet nH_2O$, $x < 1$) and copper pitch/wad, as detailed in the next sections, are better characterized as mineraloids consisting mainly of Cu, Mn, and Si and sharing similar characteristics, including a pseudo-amorphous component in the structure.

Chrysocolla

Although already mentioned by Theophrastus (315 BC) (Caley and Richards 1956) and having been the object of numerous detailed studies, no consensus has been reached yet in the scientific mineralogical community about the crystallographic structure of chrysocolla. Chrysocolla was accepted in 1969 as an official mineral phase (Fleischer 1969) with an orthorhombic lattice and an unknown spatial group (Chukhrov et al. 1968). Based on infrared observations, an intermediate structure between sheets and mono-chains was proposed (Oosterwyck-Gastuche 1970). Other authors consider chrysocolla to be a mixture of an amorphous material with an unknown cryptocrystalline phase (Schwartz 1934; Sun 1963; Newberg 1967). An attempt to characterize chrysocolla using XAFS (Farges et al. 2006) concluded to the presence of spertiniite ($Cu(OH)_2$). In contrast, Frost et al. (2012) and Frost and Xi (2013) excluded the presence of spertiniite in their samples by using thermogravimetric, XPS, and Raman analysis. The X-ray diffractogram on chrysocolla is characterized by the absence of distinct diffraction peaks (Prosser et al. 1965; Frost et al. 2012; Frost and Xi 2013) and by the appearance of a general pattern with humps at characteristic positions, similar to other ill-defined "X-ray amorphous" minerals like ferrihydrite and schwertmannite (Dold 2003a) or silicates like opal (Lynne et al. 2005).

As a logical consequence of the lack of a defined structure, the chemical composition of chrysocolla, including

its water content, is variable. This was already pointed out by Foote and Bradley (1913), who wrote that observations made on chrysocolla are "not in accord with the view that every mineral is a definite chemical compound, but it accounts for the fact regarding composition, in a way that no definite formula can do." Chemical analysis shows that in addition to the main elements Cu and Si, up to 7.3 wt% Al_2O_3 is found in chrysocolla, but generally around 1wt% (Sun 1963; Prosser et al. 1965; Newberg 1967; Oosterwyck-Gastuche 1970; Campos et al. 2015). Traces of Ca, Co, Fe, K, Mg, Mn, Na, and Pb, among other elements, are frequent and reflect the chemical environment in which it precipitates. The color of chrysocolla changes from cream white to deep blue or green. QEMSCAN® data from Campos et al. (2015) show that the chemical composition of chrysocolla varies even at a small scale.

Newberg (1967), based on experimental data, suggested that the precursor of chrysocolla is a gelatinous silica polymer issued from the saturation of silica in solution (> 100–140 mg/L Si). Newberg (1967) also stated that the presence of copper ions in solution (i.e., Cu^{2+}, $CuOH^{+}$) inhibits the formation of amorphous silica. Hariu et al. (2013) synthesized a hydrated Cu-Si gel with nearly identically XRD patterns as their chrysocolla sample from Chuquicamata. They precipitated it from a sol–gel stock solution with a Cu/Si molar ratio of 1.0 and concentrations of 8.4 g/L Cu and 3.7 g/L Si. Additionally, Cu/Si molar ratios of 0.5 and 2 were tested. The precipitation was induced by pH increase. With a Cu/Si molar ratio of 0.5, i.e., with Si excess, the resulting XRD results suggest the presence of amorphous silica. With a Cu/Si molar ratio of 2, i.e., with Cu excess, the resulting XRD pattern of the gel suggests the presence of planchéite. The final Cu/Si molar ratios in the precipitates were 0.32, 0.83, and 1.61, respectively. The color of the gels changed from sky blue to dark blue with increase of the copper content (Hariu et al. 2013). Gelatinous copper-rich material was described from several deposits (Moreton 2007; Majzlan 2020) and was also studied in detail in Exótica (Lambiel 2013; Lambiel et al. 2022).

Copper wad and copper pitch

Used as a descriptive term by miners (similarly to "limonite" for the iron oxide family), copper wad designates a dark brown to black earthy material forming patinas and cements and consisting mainly of copper and manganese with variable amounts of silica. This term is complementary with the term copper pitch, which describes a similar but massive material that shows conchoidal fracturing (Guild 1929). Copper pitch is described by Schwartz (1934) as a frequent but "impossible to define" material consisting of a mixture of copper oxides, manganese oxides, silicate, and water-forming banded structures with chrysocolla, concentric shells, and nodules.

X-ray diffraction, scanning electron microscopy, and electron probe microanalysis show that copper wad from exotic mineralization at El Salvador (Chile) contains significant proportions of cryptomelane and birnessite (Mote et al. 2001). X-ray diffraction on copper pitch from Inspiration Mine (Arizona) yields patterns indistinguishable from those of chrysocolla, what led Throop and Buseck (1971) to define copper pitch as chrysocolla colored by the presence of Mn and/or Fe. QEMSCAN® studies of Menzies et al. (2015) illustrate the chemical variability of copper wad and copper pitch, with, in addition to Cu, Si, and Mn, significant amounts of Mg, Al, Fe, Si, P, Ca, Cl, and S. Other authors define copper wad and copper pitch as "black copper silicates," both without defined structure and with a similar chemical composition (Pincheira et al. 2003).

Methodology

A total of 74 samples, 40 with copper wad and copper pitch, were collected in 2010 and 2011 in the supergene profile of the southernmost part of the Chuquicamata deposit and in the Mina Sur (Exótica) open pit (Fig. 2, ESM Fig. A1). Samples from the northern part of the Mina Sur open pit (Fig. 2) are from strongly mineralized areas which were mined during sampling, whereas those from the southern part correspond to marginal mineralization remaining after exploitation. Sampling was additionally performed in 11 drill cores on two east–west sections (Fig. 2).

Copper wad and copper pitch patinas and massive aggregates were separated manually under the binocular lens. It was possible to separate reasonably pure copper wad in 17 samples (Table ESM A3). Five samples of copper pitch were analyzed as well (Table ESM A3). UniQuant® X-ray fluorescence spectrometry was used to obtain a semi-quantitative chemical characterization of the separated material. The analyses were carried out on the Philips PW2400 vacuum X-ray fluorescence spectrometer of the Department of Earth and Environmental Sciences, University of Lausanne, Switzerland.

Powder samples were prepared for the X-ray diffraction, principally to study chrysocolla and copper wad, and in general to determine the minerals associations in the Exótica deposit. The diffractometer used was a Bruker D8 Advanced theta/2theta machine with a 2D detector (wave length 1.5406 Å, Cu K α1, step size 0.00787°theta, step time 185 s, rotation of the sample handler 15 turns/s) (Crystallography Laboratory, University of Geneva, Switzerland). Thirty open pit and drill core samples were analyzed by in situ micro-fluorescence spectrometry (μ-XRF) with an Eagle III μ-XRF instrument (Department of Earth Sciences,

University of Geneva). The qualitative element distributions and variations in cements, impregnations, and patinas of copper wad and in the copper pitch veins (Tables ESM A2 and A3) were studied. Semi-quantitative chemical data and mineral textures were obtained by SEM–EDS on thin sections and on copper wad patinas (Jeol JSM 7001F at 15 kV; Section of Earth and Environmental Sciences, University of Geneva).

All the previously mentioned methods have the limitation of providing bulk data on copper pitch and copper wad. However, as indicated above, both phases are mixtures of a probably pseudo-amorphous and chemically variable material with crystalline phases. For this reason, we have applied sequential extractions to dissolve in subsequent steps different mineral phases and mineral groups. To apply this method to copper pitch- and copper wad-bearing samples, the seven-step sequential extraction protocol of Dold (2003b) was modified by adding a supplementary step targeting specifically the manganese oxides and hydroxides (hydroxylamine hydrochloride, 0.25 M, pH 2, for 2 h). This modified sequential extraction protocol targets the following minerals and mineral groups: step 1 liberates the water-soluble fraction (1.0 g sample in 50 mg deionized water, shaken at room temperature for 1 h). Step 2 (1 M NH_4-acetate, pH 4.5, shaken at room temperature for 2 h) addressed exchangeable ions and carbonates. Step 3a (hydroxylamine hydrochloride, pH 2, shaken for 2 h) dissolves Mn oxides and hydroxides. Step 3b (0.2 M NH_4-oxalate, pH 3.0, shaken for 1 h in darkness at room temperature) dissolves the low-crystalline Fe(III) oxyhydroxide fraction, e.g., schwertmannite, ferrihydrite, and partly secondary jarosite. Step 4 (0.2 M NH_4-oxalate, pH 3.0, shaken for 2 h at 80 °C) was used to address the high-crystalline Fe(III) oxide fraction like goethite, higher ordered jarosite, and hematite. Step 5 (H_2O_2 35%, shaken for 1 h) oxidizes organic matter or secondary copper sulfides. Step 6 ($KClO_4$ and HCl) dissolves primary sulfides, and the final step 7 (HNO_3, HF and $HClO_4$) dissolves the residual fraction (mainly silicates, zircon, rutile).

The leach solution of each extraction step was analyzed by inductively coupled plasma–mass spectrometry (ICP-MS). Solutions were filtered (0.2 µm) and acidified with suprapure HNO_3 (1%). Between two steps of extraction, the sample was dried and analyzed by XRD to identify the dissolved phases by sequential X-ray diffraction (SXRD) following the method described by Dold (2003a). Two samples from Exótica considered to be pure were selected for this study (binocular lens observation and XRD verification after the selection). The first sample is a chrysocolla sample (MC24), and the second one (MC26) is a copper pitch sample, from the northern part of the deposit. The XRD patterns of each powder sample before and after the application of the sequential extraction process were compared. The experiment was run in triplicate.

To model the interaction between the solutions and the host rock during the formation of the mineralization at Exótica, the geochemical code PHREEQC (Parkhurst and Appelo 2013) was used. The llnl database was complemented with data for additional minerals including rhomboclase (Majzlan et al. 2006), libethenite, and pseudomalachite (Majzlan et al. 2015) and montmorillonite (Vieillard 2000).

Results

Mineral distribution and cross-cutting ore textural relationships

The Exótica deposit has an elongated shape extending from the southernmost part of the Chuquicamata open pit (2000 N) (Figs. 1 and 2, ESM Fig. A1) southwards through the Exótica valley, first in N-S and then NW-SW direction (0 to − 2000 N). Combining our observations with the information of the previously exploited southern parts reported by Münchmeyer (1996), the following general distribution of the dominant mineral associations along the Exótica valley can be outlined (Figs. 1 and 2):

(a) Kaolinized and mineralized bedrock. The bedrock underlying the gravels is strongly kaolinized; chrysocolla is impregnating the underlying unaltered bedrock. The kaolinized bedrock has low Cu concentrations compared to the chrysocolla-impregnated bedrock. Kaolinization and mineralization of the bedrock are particularly developed in the northern part of the deposit, i.e., close to the source of ARD in Chuquicamata (Fig. 2). Although in the literature this kaolinization has been named "argillic" (Mortimer et al. 1978; Münchmeyer 1996), we prefer to avoid this term to prevent confusion with hypogene hydrothermal alteration at the Chuquicamata porphyry copper deposit.

(b) Cemented Cu-Mn zone in strongly altered gravels. Overlying the kaolinized bedrock, the richest copper mineralization (in places > 30 wt.% Cu) occurs in the northern part of the deposit. Copper occurs mainly as chrysocolla, copper pitch, copper wad, and atacamite (Fig. 3A and C) in strongly altered gravels as pore space cement or as massive layered sequences of chrysocolla and copper pitch (Figs. 2 and 3). The fabric of this mineralization is massive, chrysocolla and copper pitch filling also the pore spaces, resulting in a low permeability rock unit. Massive chrysocolla intercalated with copper pitch is particularly found in the lower center part of the vertical mineralization stratig-

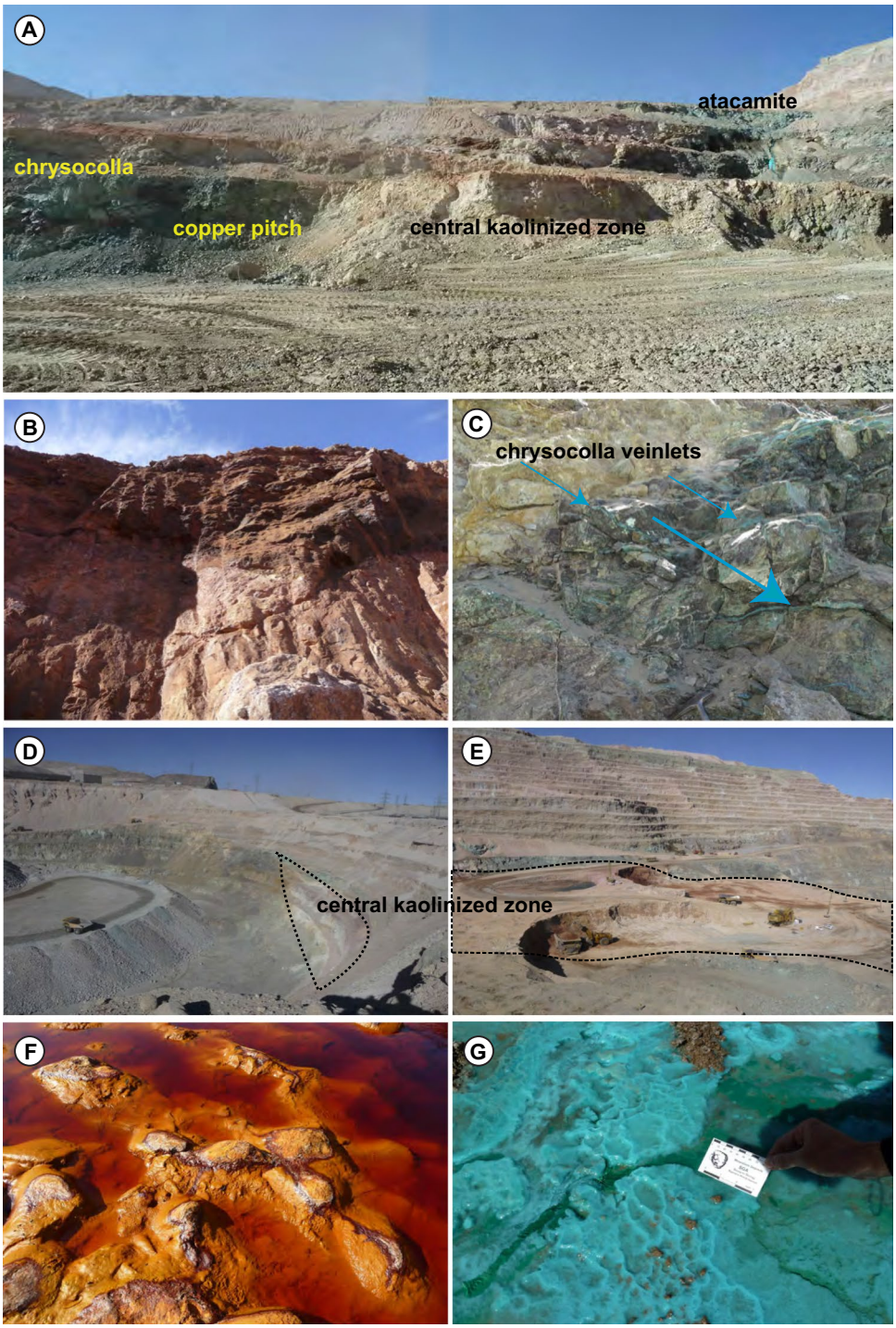

Fig. 3 **A** West–east view of the northern part of the Exótica pit during the final stage of exploitation (2011). In the central part dominates the strongly kaolinized central zone. Towards the left, massive copper pitch (black) is in contact with chrysocolla (light blue) in unaltered gravels. On the right upper part, greenish atacamite in unaltered gravels is visible. **B** Zoom of the upper kaolinized central zone with patinas of Fe(III) hydroxides. **C** Contact of massive copper pitch with the kaolinized zone, showing that the kaolinization overprints the copper pitch that is partly dissolved and re-precipitated as secondary chrysocolla veinlets. **D** W–E view in the southern part of the Chuquicamata pit, showing the central kaolinized zone with copper pitch and chrysocolla mineralization at the borders. **E** The kaolinized central zone in the northern part of the Exótica pit. **F** and **G** represent modern equivalent systems how the precipitation of the Cu-Mn-Si mineralization might have occurred. **F** Modern ARD system of Rio Tinto, Spain, with schwertmannite/goethite precipitation from the acid Fe, SO_4-rich ARD cementing the gravels in the riverbed. **G** Surficial drainage outcrop in Exótica 2011 with the precipitation of Cu-rich gel containing schulenbergite and spangolite (Lambiel et al. 2022). The formation of chrysocolla/copper pitch mineralization is thought to have been taken place in a similar flow regime but dominated by bluish and black colors

raphy overlying the bedrock. In the upper part of the sequence, atacamite, commonly together with gypsum, is present, mainly in fractures cross-cutting the previous mineralization (Figs. 4 and 5). This cemented Cu-Mn zone is only found in the northern part of the Exótica valley, whereas further south, it changes into dominantly chrysocolla/copper wad, without copper pitch, in strongly kaolinized gravels.

(c) Massive chrysocolla in unaltered gravels. Laterally of the Cu-Mn zone, as well as in the southern part of Exótica, chrysocolla is present as massive pore space fillings in unaltered gravels (Figs. 2A and B and 3A). Only at the very southern margin of this mineralization zone was a minor copper wad rim observed.

(d) Strongly kaolinized central zone. In the upper central to eastern part of the valley, a strongly kaolinized

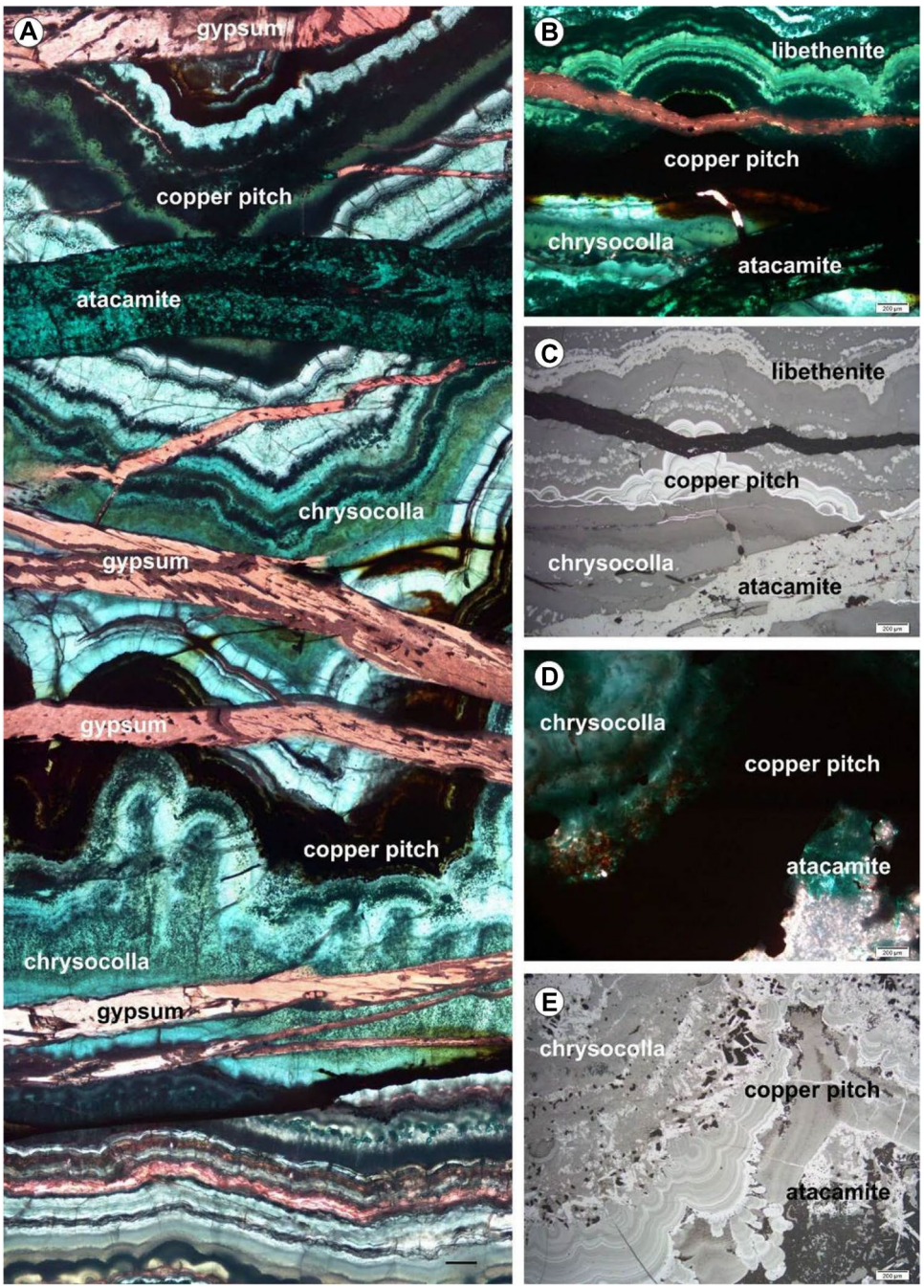

Fig. 4 **A** Transmitted light, plane-polarized, sample MC41, massive chrysocolla–copper pitch cross-cut by atacamite and gypsum veins. **B** Transmitted light, plane-polarized, sample MC41, chrysocolla–copper pitch massive mineralization, with libethenite in the chrysocolla, cross-cut by gypsum, and atacamite veins. **C** Same area as **B** in reflected light, plane-polarized. **D** Transmitted light, plane-polarized, sample MC25, massive copper pitch chrysocolla with atacamite and gypsum (white). **E** Same area as **D** reflected light, plane-polarized showing that two generations of copper pitch are present, one of botryoidal texture and a posterior massive copper pitch pore space filling

zone forms a "channel" of strongly altered gravels and underlying bedrock (Fig. 2 and Fig. 3A). X-ray diffraction shows that the mineralogy of this part of the system consists mainly of kaolinite, montmorillonite, iron oxides (goethite), and some Fe-Al-K oxyhydroxy sulfates (jarosite, alunite), as well as gypsum produced by the interaction of the gravels and bedrock with acid solutions. Relict quartz and sericitized feldspar from the hypogene assemblage could also be observed. Strongly altered samples contain lower copper concentrations (CuO between 0.1 to 0.6 wt%, with some values up to 1.0 wt%) (ESM Table A4) than the mean grade of the deposit (1.17% Cu) (Ossandón et al. (2001)). Manganese content is generally below the detection limit, except in certain iron-rich samples that yield up to 0.3 wt% Mn. The strong alteration results in a degradation of the grain size that contributes to the low permeability of the kaolinized central zone.

As seen in Fig. 3C, the strongly kaolinized central zone overprints in places the Cu-Mn zone. Copper contents between 0.4 and 0.7 wt% Cu, with values up to 1.1 wt% and manganese up to 0.5 wt%, are significantly

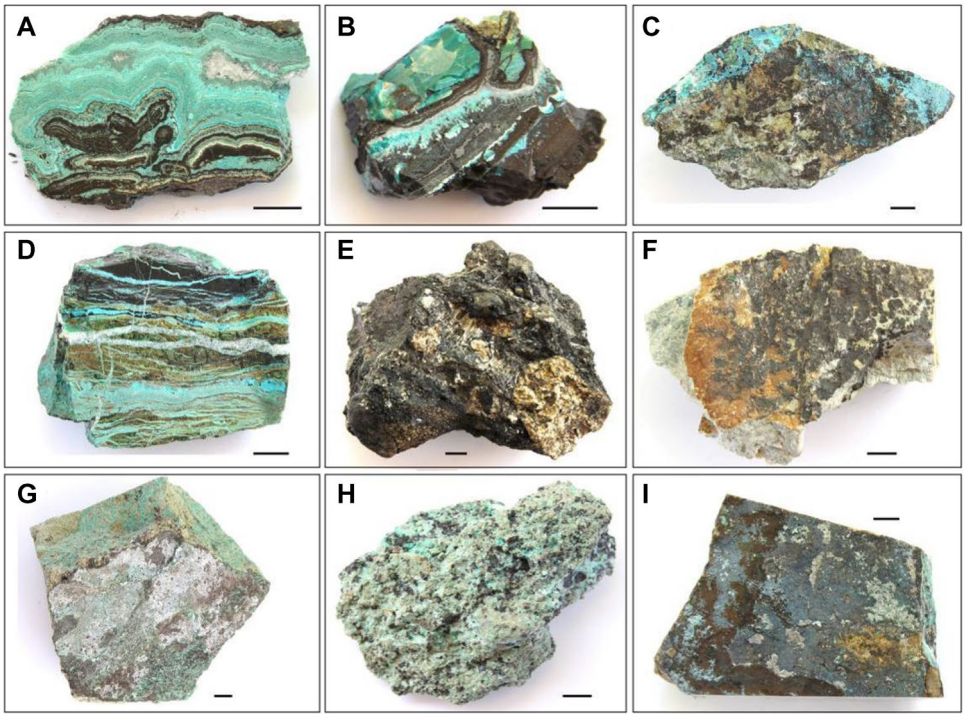

Fig. 5 Representative chrysocolla (light blue), copper pitch (black), and copper wad samples (locations indicated in ESM Figs. A.1, A.2). **A** M10.2, massive sample of chrysocolla, copper pitch, and gypsum, sampled at the contact between bedrock and gravels, east of N600 section. The sample has on top of the upper copper pitch layer a powdery patina consisting mainly of copper wad. **B** M107, massive sample of copper pitch, chrysocolla, and gypsum (white). **C** M44.2, rock clast coated by patina made of copper wad, chrysocolla, and gypsum. North of Exótica mine. **D** MC27, massive sample consisting mainly of chrysocolla (light blue) copper pitch (black) and a mixture of chrysocolla and atacamite and copper pitch. The white horizontal and vertical veins are mainly gypsum partly postdating atacamite (see Fig. 3), unknown location in Exótica deposit. **E** M33, gravels cemented with copper wad from the southwest of Exótica. **F** M40.1, bedrock piece with copper wad and iron oxides patina, from the north of the Exótica deposit. **G** M17.2, bedrock piece with copper wad, atacamite, and gypsum patina, from the west of section N600. **H** M07.1, gravel cemented with chrysocolla and small patches of copper wad, from the north of Exótica deposit. **I** M48, bedrock piece with a patina of copper wad, chrysocolla, and gypsum, from the north of the Exótica deposit. Size of the scale bar in the figures is 1 cm

lower than in the Cu-Mn zone and are characteristic for these "transitional" zones. Element mapping shows that copper occurs both as rims in iron-rich material and disseminated within the altered material (Pinget 2016). It has not been possible to attribute the copper concentrations to specific mineral phases; possibly, it is co-precipitated with Fe(III) oxyhydroxides (Fig. 3B) and/or adsorbed to particular clay minerals like montmorillonite, due to their low point of zero charge (PZC), or fixed due to cation exchange.

(e) Atacamite/brochantite occurs along the N-S trending Exótica valley mainly as massive pore space filling or impregnation of the former Cu-Mn zone, dominantly in the upper part of the mineralization where unaltered gravels prevail. It can also impregnate the lateral parts of unaltered gravels in deeper levels. Münchmeyer (1996) reported that atacamite was mainly associated to the upper portion of the northern part of the deposit cementing preferentially unaltered gravels or filling pore spaces in the preexisting mineralization. Petrographic study and SEM backscattered electron imaging show that atacamite veins always cut the previous Cu-Mn mineral assemblages (Fig. 4), indicating that atacamite precipitation is the latest event in the ore formation process and its precipitation is not accompanied by alteration of the preexisting Cu-Mn mineralization. Gypsum occurs associated to atacamite/brochantite veins or as pure gypsum veinlets cross-cutting the atacamite veins (Fig. 4).

The Cu-Mn zone with massive mixed layers of chrysocolla and copper pitch (Figs. 4 and 5A–D) is mainly observed in the northern part of the Exótica deposit. In the central part of Exótica, copper wad and chrysocolla occur mainly as open space filling, particularly as intergranular cement and as patina covering clasts and bedrock fissures. In places, copper wad and chrysocolla also impregnate basement rocks and sediments (Fig. 5E–I). Micro-fluorescence analyses also allowed to observe the textural relationship

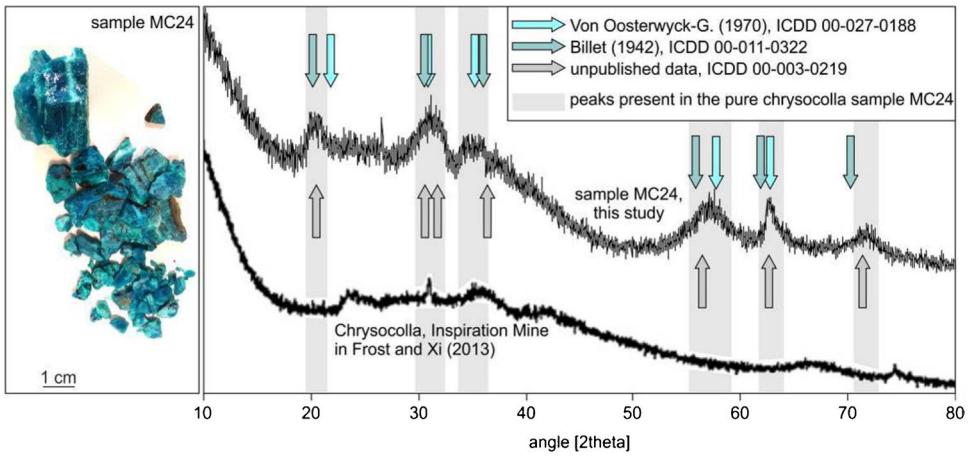

Fig. 6 X-ray diffractogram of the pure chrysocolla sample MC24. For comparison, also the diffractogram of chrysocolla of the Inspiration Mine presented by Frost and Xi (2013) is shown

between the clasts/bedrock and the copper wad mineralization (ESM Fig. B4). Copper wad typically cements fractures and fills open spaces and only rarely impregnates the sediments or the bedrock, in places along fractures.

South of 1200S, the mineralization is characterized by the dominance of chrysocolla cementing unaltered gravels; south of 2200S, copper wad dominates as surface patinas and open space filling of the gravels (Münchmeyer 1996).

Mineralogical and geochemical characterization of chrysocolla, copper pitch, and copper wad

Chrysocolla ($Cu_{2-x}Al_x(H_{2-x}Si_2O_5)(OH)_4 \cdot nH_2O$, $x < 1$) XRD analyses show the typical signature of pseudo-amorphous material with "humps" instead of well-defined peaks as it has been described before (Figs. 6 and 7). Figure 6 shows the XRD pattern obtained from the purest chrysocolla sample from Exótica (MC24). The principal hump at around 21.5° (2θ) (Billiet 1942; Oosterwyck-Gastuche 1970) is also characteristic for opal-A (Nicolau et al. 2014). Other humps already described as characteristic for chrysocolla by Billiet (1942), Oosterwyck-Gastuche (1970), or Frost and Xi (2013) are also present in the diffractogram of Fig. 6. XRD carried out by Frost and Xi (2013) in the Inspiration Mine indicates that chrysocolla may show patterns with less marked humps (Fig. 6).

The chemical composition of chrysocolla from Exótica (Fig. 8, ESM Table A3) is in agreement with other published analyses of this mineral (Chukhrov et al. 1968; Crane et al. 2001), with CuO between 36 and 47 wt%, SiO_2 between 37 and 43 wt%, and Al_2O_3 up to 3.3 wt% (Fig. 8). Smaller

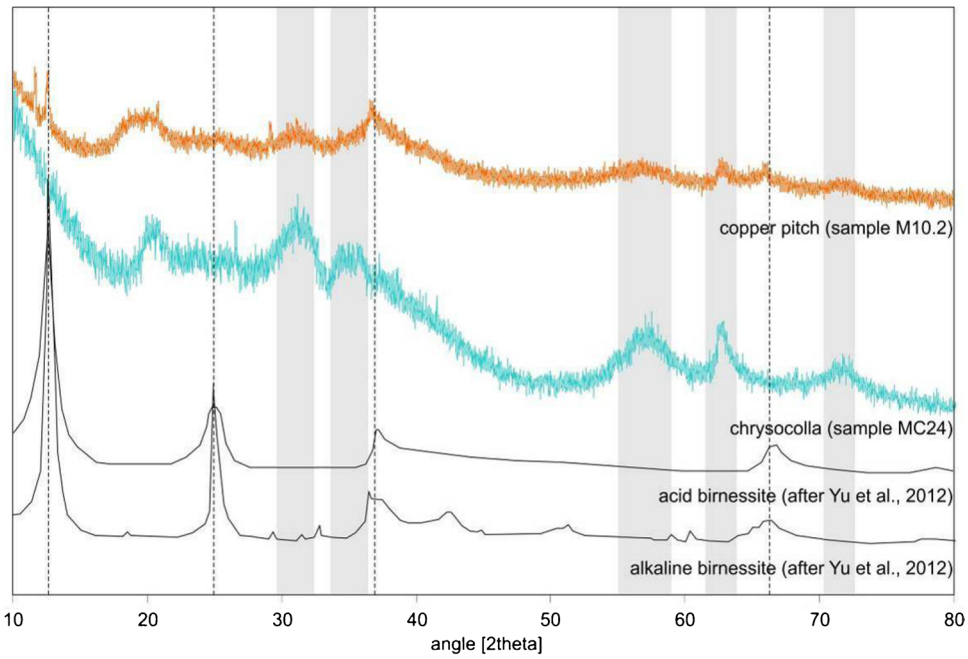

Fig. 7 XRD patterns obtained on samples M10.2 (pure copper pitch) and MC24 (pure chrysocolla) compared to the pattern obtained on acid and alkaline birnessite samples by Yu et al. (2012). The comparison indicates more similarities between the birnessite contained in the copper pitch with the acid birnessite than with the alkaline birnessite, supporting the hypothesis that the copper pitch of Exótica was formed under acid conditions

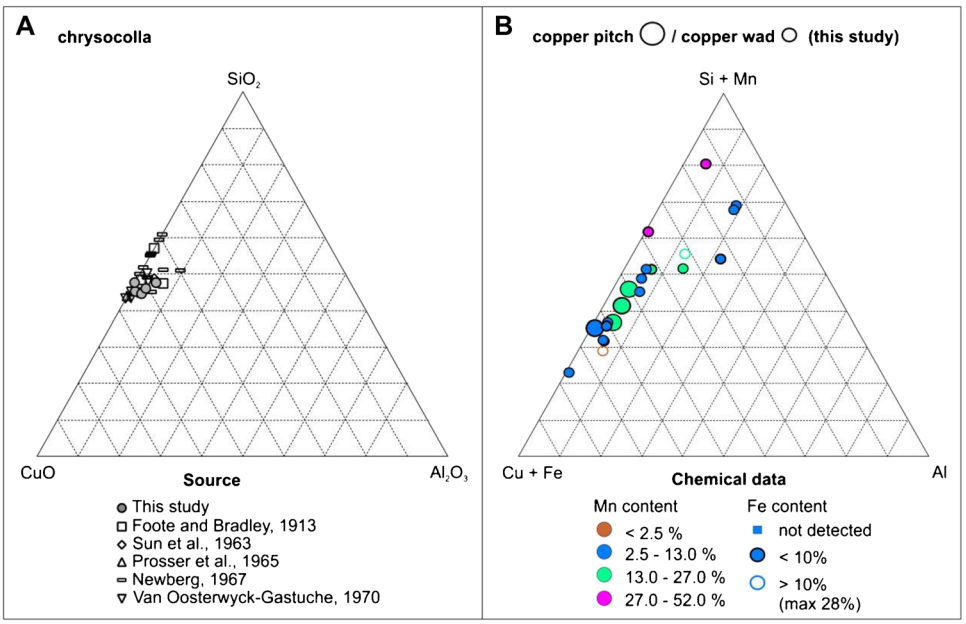

Fig. 8 **A** $CuO\text{-}SiO_2\text{-}Al_2O_3$ plot of chrysocolla (data in ESM Table A.4). **B** Results of the XRF analyses for copper wad and copper pitch, presented in a Cu + Fe-Si + Mn-Al triangular diagram. Si and Mn are roughly linearly related, as illustrated with the symbol colors. The iron concentration is generally not relevant in comparison to the copper concentration, apart for the two samples signalized with empty symbols. The size of the symbols makes the difference between copper pitch and copper wad

amounts of other elements were detected including Mn (0.3 to 0.7 wt%), Fe (0.2 to 6.2 wt%), Ca (0.7 to 1.1 wt%), S (0.3 to 1.1 wt%), K (0.1 to 0.4 wt%), Cl (0.06 to 5.2 wt%), Zn (0.05 to 0.34 wt%), and P (0.07 to 0.31 wt%).

Copper pitch XRD analyses of copper pitch samples show patterns similar to those obtained for chrysocolla, except for the presence of peaks attributed to birnessite ($(Na,Ca)_{0.5}(Mn^{4+},Mn^{3+})_2O_4 \bullet 1.5H_2O$) (Figs. 7 and 9). The obtained peaks from our samples are similar to those of birnessite precipitated under acidic rather than alkaline conditions according to the experiments performed by Yu et al. (2012), that indicate that the alkaline birnessite has abundant secondary peaks which are missing in the acid birnessite (Fig. 7). Copper pitch at Exótica is composed mainly of Cu (3 to 47 wt%), Si (7 to 25 wt%), Mn (1.5 to 37 wt%), Al (0.2 to 11 wt%), and Fe (0.2 and 28 wt%) (Fig. 8, ESM Table A3).

Copper wad Copper wad occurs commonly with gypsum, iron oxides, chrysocolla, atacamite ($Cu_2(OH)_3Cl$), and libethenite ($Cu_2(PO_4)(OH)$). The textural relationships between these minerals were investigated with SEM secondary electron imaging (ESM Fig. B1). The signature of the pseudo-amorphous copper wad is obscured by the presence of small amounts of well crystallized minerals (ESM Figs. B2 and B3) that prevent its characterization by XRD. In addition to the host rock minerals (principally quartz and feldspars), gypsum, atacamite, paratacamite, and birnessite were identified in the XRD analyses.

Micro-fluorescence results on copper pitch and chrysocolla illustrate the distribution of Mn, Fe, and Cu and how the variations of chemical composition affect the color of the sample (ESM Figs. B4). Manganese gives a black color to the material and iron, probably as Fe^{2+}, a more greenish tint. In the absence of manganese and iron, the color is the typical light blue color of chrysocolla.

High-resolution mineralogical and geochemical characterization by sequential extractions combined with sequential XRD (SXRD)

In order to decipher the mineralogical and geochemical composition of chrysocolla and copper pitch, a combination of sequential extraction and XRD after each leach (SXRD) was applied to two selected samples (Fig. 9). The chemical compositions (ICP-MS; ESM Table A1) of the leach solutions of each dissolution step are shown in Fig. 10. The XRD pattern of the chrysocolla sample (MC24) corresponds to almost pure chrysocolla (Figs. 6 and 9); only a small peak located at 26.7° 2theta indicates minor quartz. In contrast, the XRD pattern of the copper pitch sample (MC26) displays several sharps peaks pointing to the presence of gypsum and atacamite (Fig. 9). The results of the sequential extraction steps are summarized as follows (Figs. 9 and 10).

Step 1. Water leach (1 h, room temperature): this first step did not affect the mineralogy of the chrysocolla sample and drastically reduced the gypsum present in the copper pitch sample as indicated by the liberation of between 3200 and 4100 mg/kg of Ca (Fig. 10, ESM Table A1). The liberated amount of Cu (31.4 mg/kg) is negligible compared to the following steps.

Step 2. 1 M NH_4-acetate (pH 4.5, 2 h, room temperature): in the chrysocolla sample, at 18.2° 2θ a new peak appeared,

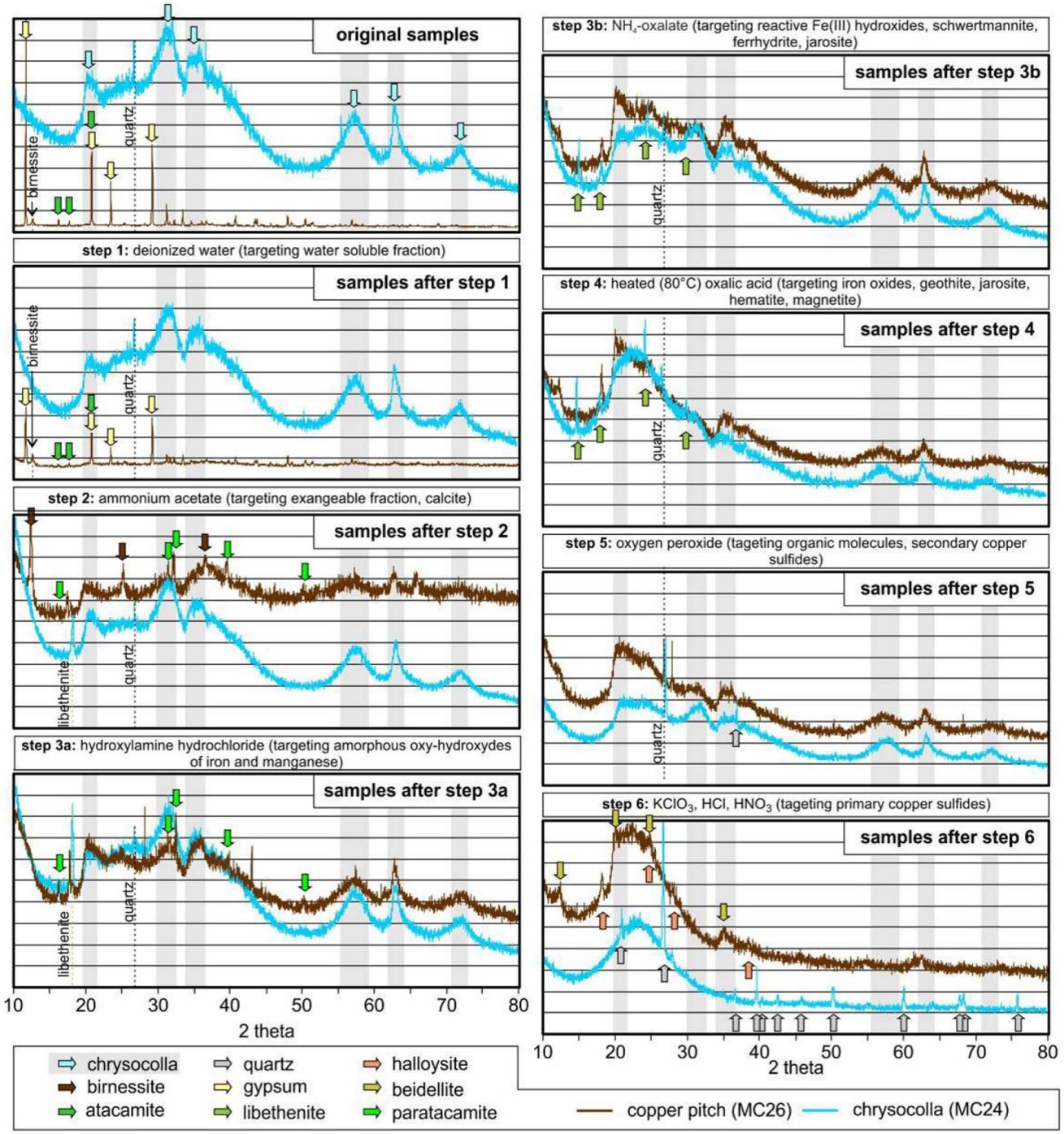

Fig. 9 Results of the XRD analyses on the chrysocolla and copper pitch samples before the sequential extraction and after each dissolution step. Arrows indicate the principal peaks of the identified mineral phases

corresponding to the main libethenite peak ($Cu_2(PO_4)(OH)$), a Cu-phosphate common in oxidation zones of copper ores, mainly derived from apatite weathering. The dissolution of gypsum and atacamite during this step may explain the appearance of this peak, as the detection limit of XRD is between 2 and 5%, depending on crystallinity. The new peak could also be due to libethenite neo-formation during extraction, but this is unlikely due to the low solubility of metal phosphates. In the copper pitch sample, gypsum and also atacamite appear to have fully dissolved, and peaks of birnessite and paratacamite ($Cu_3(Cu,Zn)(OH)_6Cl_2$) appear. The ICP-MS analyses on the solution resulting from

the dissolution step 2 (Fig. 10) are consistent with these observations.

Step 3a. Hydroxylamine hydrochloride (pH 2, 2 h): this leach does not affect the XRD pattern obtained on the chrysocolla sample where the libethenite peaks remain. In the copper pitch sample, XRD evidences the dissolution of birnessite, whereas paratacamite remains stable. The color change of the copper pitch sample from dark brown to green illustrates the loss of manganese. This color change indicates that the dark brown to black color of copper pitch is due to the presence of birnessite. The geochemical data from the sequential extractions confirm these findings (ESM Table A1) (about 1000 mg/kg Cu and 150 mg/kg Mn in the chrysocolla sample, and about 3700 mg/kg of Cu and 4500 mg/kg of Mn in the copper pitch sample) (Fig. 10) and suggest that an important amount of Cu is associated to birnessite. After this step, a similitude of the XRD pattern of the copper pitch sample with that of chrysocolla is recognized (Fig. 9).

Step **3b.** 0.2 M NH_4-oxalate (pH 3, 1 h, dark, room temperature): the characteristic XRD pattern of chrysocolla starts to degrade. The leach does not dissolve any crystalline phase in the chrysocolla sample. During acidification of the solutions issued from the sequential extraction steps 3b and 4 on samples of chrysocolla and copper pitch, a blue precipitate consisting mainly of copper formed in the test tubes, most likely Cu oxalate complexes (over 98% for the chrysocolla and over 97 wt% for the copper pitch sample, both in steps 3b and 4, semi-quantitative XRF analyses).

The element concentrations listed in ESM Table A1 were corrected taking in account the precipitate formed after acidification of the given sample. The dissolution of amorphous material is suggested by the liberation of important amounts of Cu (up to 42,000 mg/kg in chrysocolla and 13,000 mg/kg in copper pitch), Al (around 860 mg/kg in chrysocolla and 320 mg/kg in copper pitch), and Si (around 240 mg/kg in chrysocolla and around 500 mg/kg in copper pitch), resulting in an increase of the libethenite peaks. In the copper pitch sample, paratacamite disappears, and the peaks of libethenite continue to be present.

Step 4. 0.2 M NH_4-oxalate (pH 3, 2 h, 80 °C): the characteristic XRD pattern of chrysocolla continues degrading. The shape of the background pattern is modified by an increase of the main hump of chrysocolla, suggesting the dissolution of amorphous phases (possibly Al and Fe hydroxides, as suggested by the relatively high concentrations of Al and Fe in this leach) (Fig. 10). Similar but less pronounced changes are observed in the copper pitch sample. Libethenite is not dissolved, and the tiny libethenite needles recognized under thin section and SEM (ESM Fig B.1F) appear to produce clear peaks in the XRD analyses, even if this mineral is present only in small amounts. The mainly released elements during this step are Si, Cu, Al, and Fe in both samples (ESM Table A1).

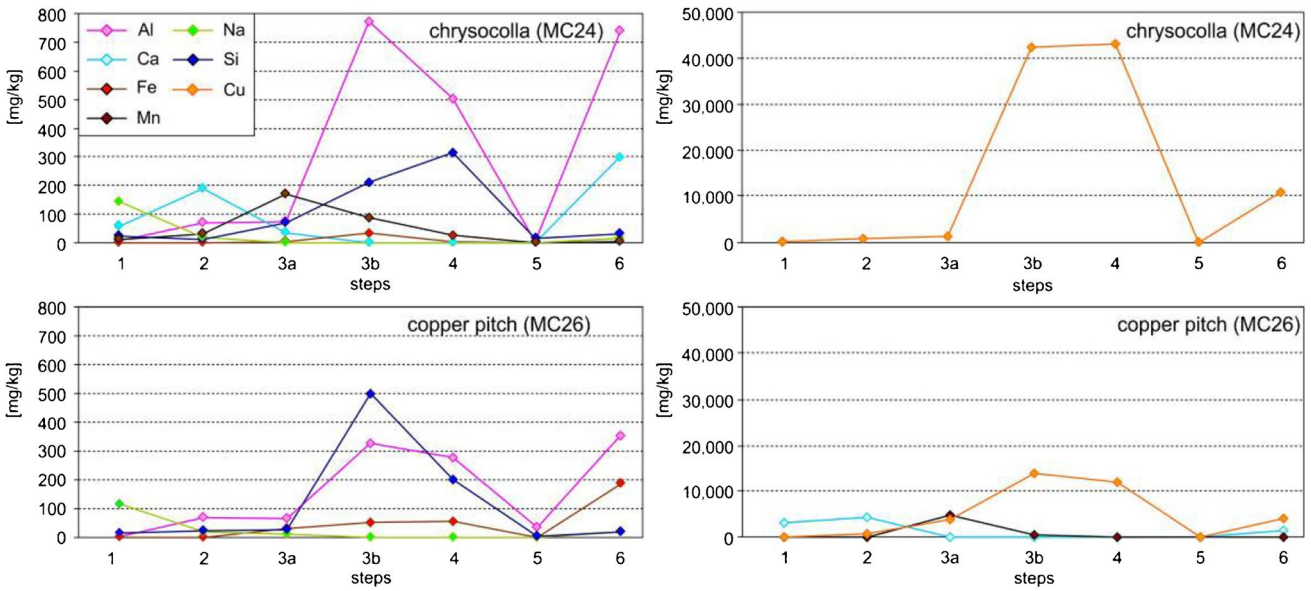

Fig. 10 Results of the ICP-MS analyses made on the solutions resulting of each extraction step for Al, Ca, Cu, Fe, Mn, Na, and Si for sample MC24 (chrysocolla) and sample MC26 (copper pitch). The results obtained after steps 3b and 4 are corrected taking in account the formation of a precipitate in the solutions during acidification. Step 3a, designed to dissolve Mn hydroxides and oxides, shows high selectivity, especially in copper pitch, while steps 3b and 4 address chrysocolla with good selectivity, shown by the complete Si dissolution after step 4

Step 5. H_2O_2 35% (1 h): the first hump of the chrysocolla pattern keeps collapsing, and the libethenite peaks disappear in both samples. Chemical data of the solutions resulting from this step show that the released amount of copper is low (between 4 and 20 mg/kg, ESM Table A1).

Step 6. $KClO_4$ and HCl: the chrysocolla XRD pattern in both samples has completely disappeared. In the chrysocolla sample, the peaks for quartz continue to be clear. In the copper pitch sample, new peaks appear, that are difficult to interpret. The pattern could indicate the presence of a clay mineral. In the context of the Exótica deposit, it could be kaolinite, halloysite ($Al_2Si_2O_5(OH)_4 \bullet nH_2O$), and/or beideite ($(Na,Ca_{0.5})_{0.3}Al_2((Si,Al)_4O_{10})(OH)_2 \bullet nH_2O$), but the small amount of available material prevented any precise identification. During step 6, the main liberated elements are Cu (between 5000 and 10,000 mg/kg in the chrysocolla sample and between 3000 and 4200 mg/kg in the copper pitch sample), and smaller amounts of Al, Ca, Fe, and other elements are listed in ESM Table A1.

Discussion

Copper pitch/wad

SXRD analysis of the chrysocolla and copper pitch samples has allowed to identify the compositional phases. In the crysocolla sample, with the use of NH_4-oxalate (steps 3b and 4), the characteristic XRD pattern of chrysocolla started to disappear, indicating that its structure collapsed. The data also showed that the sample contained small amounts of libethenite and quartz, the former becoming visible under XRD, when chrysocolla started to dissolve. In the copper pitch sample, the presence of crystalline phases mixed with copper pitch masks the typical XRD pattern of chrysocolla. After the dissolution of gypsum and atacamite (step 2), the chrysocolla XRD pattern and the libethenite peaks appear; and the similitude of the XRD patterns of chrysocolla and of copper pitch becomes evident. Thus, SXRD shows that copper pitch/wad consists in essence of chrysocolla with co-precipitated birnessite and/or amorphous Mn oxide phases. Further, the use of SXRD allows the identification of additional trace minerals that are typically camouflaged by more abundant minerals in the XRD pattern before the successive leaching steps.

Geochemical modeling of the formation conditions of the Exótica mineral assemblage

The geochemical interaction of Cu-Mn-Si in solution was modeled with PHREEQC (Parkhurst and Appelo 2013) at 25 °C in order to interprete the observed associations and textures of chrysocolla, copper pitch, and copper wad and understand the geochemical conditions under which they formed.

As shown above, copper pitch and copper wad are complex mixtures with variable geochemical composition (Fig. 8). In order to simplify the geochemical modeling, both copper pitch and copper wad were considered to be a mixture of chrysocolla and birnessite. When both minerals reach supersaturation in the model, it is assumed that copper pitch/wad precipitates. However, it has to be stated that this approach gives only indicative geochemical conditions in which the copper pitch/wad may form, as no thermodynamic data are available for the amorphous phases detected.

To approach the geochemical border conditions at which the mineral assemblage chrysocolla–birnessite could form, a simulation series was performed with Eh between 0.1 and 0.9 V: 0.001–1 g/L Cu and Mn and 0.001–10 g/L Si (ESM Figs. B5 and B6). These concentrations were chosen between those used by Hariu et al. (2013) in stock solutions of hydrated copper silicate gels, considered to be a synthetic analogue for Chuquicamata chrysocolla (in the range of g/L for Cu and Si), and those in the range of mg/L for Cu and Si encountered in waters in contact with neo-formed Cu-gels in the Exótica pit (Lambiel et al. 2022). The results of the modeling (ESM Figs. B5 and B6) indicate that chrysocolla precipitation strongly depends on the silica concentration in solution, as already observed by Newberg (1967). During the formation of the Exótica deposit, the strong alteration of the silicate assemblage due to ARD interactions is the main source of dissolved Si. This mechanism has been shown in laboratory experiments in copper tailings leached by diluted sulfuric acid, where after the leach-out of the metal content Al and Si are liberated into solution through silicate weathering at continuously low pH (Jurjovec et al. 2002). The same authors show that addition of natrojarosite to the tailings accelerates pH decrease and element release (Jurjovec et al. 2003).

Our geochemical modeling has shown that copper and manganese concentrations also have important influence on the saturation indices of chrysocolla and birnessite (ESM Figs. B5 and B6). The findings of these simulations are summarized in Fig. 11. Chrysocolla is stable at pH values above ~ 5 and below 9 and at oxidizing conditions (Eh > ~ 0.1 V), whereby redox variations have a smaller impact than for birnessite (Fig. 11A). The solubility boundary of the birnessite stability field increases linearly to higher Eh with decreasing pH (Fig. 11A). Mn has low solubility in oxic acidic conditions, while it shows high solubility under reducing and acid to neutral conditions. Increasing Cu and Mn concentrations expand the stability field of both minerals towards lower pH (Fig. 11A). Thus, the stability field in which copper pitch/wad can precipitate (i.e., the field of chrysocolla and birnessite co-precipitation) ranges from Eh above 0.5 V and pH between 4.5 and 7 approximately. With slightly lower redox potential, only chrysocolla will precipitate, and with lower pH

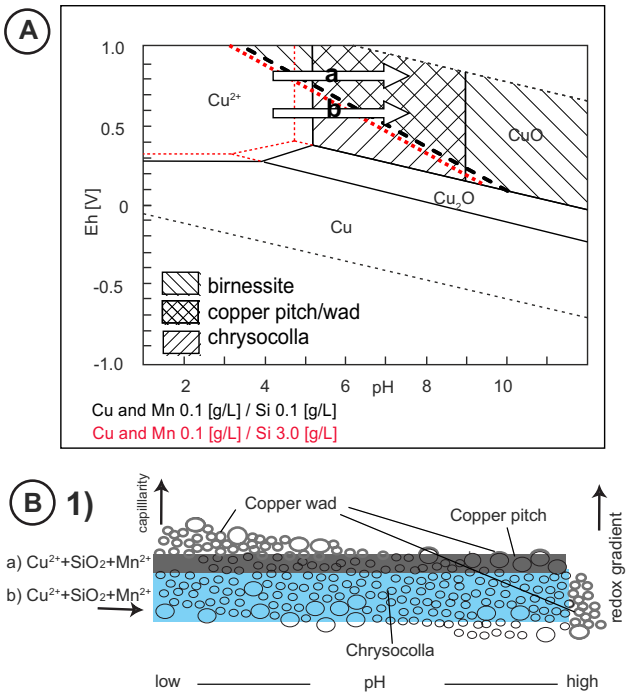

Fig. 11 **A** Eh–pH diagram for Cu-Si-Mn system at 25 °C showing the stability fields of chrysocolla and birnessite. Where both stability fields overlap, the conditions for copper pitch/wad formation are given. Increased Si concentrations result in expansion of the stability field towards acidic pH (red dotted lines). Arrow a shows the pathway at very oxidic condition (i.e., superficial flow or unsaturated gravels, where birnessite (i.e., copper pitch/wad) can precipitate at low pH. Arrow b shows the sequence under slightly more reducing conditions: first chrysocolla precipitates and only if the pH reached the required higher pH values also birnessite can precipitate and copper wad can form, as, for example, in the southernmost part of the Exótica deposit. **B1** Schematic model of the mineralization sequence and environment of the copper pitch/wad formation under oxic conditions and chrysocolla–copper wad from Cu-Mn-Si rich solution in reducing conditions (groundwater flow in gravels)

and higher Eh, only birnessite (Fig. 11A). An increase of the Si concentration results in a significant expansion to the chrysocolla stability field towards lower pH but does not affect importantly the conditions of precipitation of birnessite (Fig. 11A). The source of Mn and Cu was the Cu-Mn-Si-dominated solutions coming from the acid drainage formed in the oxidation zone of the Chuquicamata porphyry deposit.

ARD in Chuquicamata can be assumed to have dissolved high Fe concentrations from pyrite/chalcopyrite oxidation and biotite weathering and Mn from dissolution of rhodochrosite and other Mn-bearing carbonates; other dissolved metal cations were dominated by Cu. During oxidation, Fe(III) hydroxides precipitated first at low pH, due to their low solubility, as, for example, jarosite-schwertmannite-goethite at the pH range of 2–4, and therefore retained most of the iron in the oxidation zone of Chuquicamata. Mn in this pH range is mainly mobile as Mn^{2+}, but can precipitate as birnessite when pH is higher than 3 with strong oxic conditions i.e., as those prevailing under superficial run-off (Fig. 11). Therefore, Mn was mainly leached out from the Chuquicamata oxidation zone towards Exótica together with Cu and anions like SO_4^{2-}, HCO_3^-, PO_4^{3-}, and $H_3SiO_4^-$, which participated as ligands for copper mineral precipitation.

Hence, the solutions that percolated into the Exótica valley can be assumed to have been mainly of low pH (~2–4) and Cu-Mn-Si-dominated. Increase of pH, due to water–rock interaction, and increase of the activity of the solutes through evaporation (Fernández-Mort et al. 2018), could trigger under oxidizing conditions (i.e., superficial flow) precipitation of copper wad/pitch (Fig. 11A-a), while under more reducing (i.e., groundwater flow), only chrysocolla could precipitate (Fig. 11A-b). Under near-neutral and slightly reducing conditions (~0.5 V), birnessite would become supersaturated again at higher pH and copper wad could form (Fig. 11A-b). This mechanism explains the minor copper wad occurrence at the most external edges of the zone of "massive chrysocolla in unaltered gravels" at the southernmost part of Exótica.

Therefore, chrysocolla and birnessite precipitation was favored by high evaporation rates, especially in ponds and superficial waterflows that increased the activities of the solutes, and so co-precipitation of chrysocolla and birnessite could form copper pitch horizons. The layering of chrysocolla with intercalations of birnessite-rich copper pitch suggests periodical flush-out of the Chuquicamata oxidation zone associated to rain events, possibly with surface run-off, where Mn was flushed out from the oxidation zone of Chuquicamata and percolated then on the surface forming copper pitch/wad. Therefore, changes in pH, redox, and solution composition produced a sequence of chrysocolla/copper pitch cemented gravels and surface layers with copper wad forming at the grain surfaces due to capillarity. Figures 3F and G illustrate modern ARD precipitates with features similar to those that possibly had chrysocolla/copper pitch layers formed in ponds and superficial waterflows during the formation of the Exótica deposit.

Additionally, layers of the copper phosphates libethenite (Figs. 4 and 9) and pseudomalachite (Kahou et al. 2021) have been identified in Exótica. They are intercalated between chrysocolla and copper pitch layers (Figs. 4B and C). The phosphate source was most likely apatite weathering in the Chuquicamata ore. In Australian deposits like Girilambone and Northparkes, pseudomalachite is mainly reported to be associated to malachite and azurite in the lower parts of supergene zones, while libethenite is associated to the upper part of the oxidation profiles where extensive kaolinization prevails (Crane et al. 2001). This is in line with the thermodynamic stability fields of both minerals, where libethenite

dominates at lower pH and higher phosphate activities, while pseudomalachite dominates at higher pH and lower phosphate and higher carbonate activities (Crane et al. 2001; Majzlan et al. 2015). The ARD solutions encountered fresh Fortuna gravels and chloritic alteration of the basement with the presence of calcite about 2.5 km from the ARD source, so that pH was slightly higher and phosphate activities were lower, suitable for pseudomalachite formation. In contrast, the northern upper part of Exótica was most likely exposed to lower pH and higher activities of phosphate due to the proximity of the oxidizing Chuquicamata ore body, producing the geochemical conditions for libethenite precipitation.

If the metal-rich solutions migrated along deeper levels of the gravels, i.e., in a more reducing environment (e.g., < 0.5 V), chrysocolla would cement first, and only at high pH (7–8), i.e., in unaltered gravels far away from the acidic source, co-precipitation of birnessite would be possible, and copper wad could form (Fig. 11). The cementation of the gravels with chrysocolla and copper pitch made them relatively impermeable and forced the following generations of solutions to migrate laterally or above the previous mineralization, with only some dissolution and re-precipitation in the contact zones. Since the deposition direction of the Fortuna gravels in the southern part of the Exótica deposit was from the northwest to the southeast, the ARD flow channel on the surface was forced to migrate towards the southeast which explains the morphology of the deposit (Figs. 2 and 12B).

If, because of previous drainage, the ARD source was depleted in Cu and Mn, then acidic, but metal-poor solutions would alter the gravels resulting in the "strongly kaolinized central zone," as observed in the southern part of Chuquicamata and the northern part of Exótica as a final stage of the leaching of the Chuquicamata oxidation profile.

Genetic model of the formation of the Exótica deposit

The key findings from the detailed mineralogical and geochemical characterization and geochemical modeling of the ore assemblage of Exótica can be summarized as follows:

- Copper pitch/wad is chrysocolla with co-precipitated birnessite and pseudo-amorphous Mn oxides/hydroxides.
- Birnessite in copper pitch at Exótica formed in an acidic environment, i.e., from ARD.
- Birnessite (constituent of copper pitch/wad) forms in a particularly oxidizing environment (e.g., superficial run-off), whereas pure chrysocolla can precipitate as well in a slightly more reducing environment (e.g., groundwater flow).
- Formation of atacamite is the latest copper mineralization event, cross-cutting all previous mineralization events.

These results combined with those published on the tectonic, sedimentary, and climatic evolution of the Calama basin in the last 35 Ma, allows us to propose a four-step conceptual genetic model for the Exótica ore formation (Fig. 12):

A. ***Formation of a mature supergene enrichment profile at Chuquicamata (~ 30–25 Ma to ~ 15 Ma) and mineralization in the bedrock of the Exótica valley (Fig.*** 12A)

Supergene processes started in the Chuquicamata-Exótica area at ~30–25 Ma (Mortimer et al. 1978), with the exhumation and erosion of the Chuquicamata porphyry copper mineralization during the Andean uplift (Fig. 12A) (Sillitoe et al. 1968; Armijo et al. 2015). The main oxidation of the sulfide mineralization at Chuquicamata continued until the onset of arid to hyper-arid conditions at ~ 15 Ma (Rech et al. 2006; Jordan et al. 2015; Armijo et al. 2015; Cooper et al. 2016; Evenstar et al. 2017) and resulted in the formation of a mature supergene profile with a leached oxidation zone, and an underlying chalcocite–covellite enrichment blanket (Pinget 2016). A mass balance study suggests that vertical 900 m of the mineralized porphyry had to be oxidized and eroded to supply the amount of supergene copper present both in Chuquicamata and in Exótica (Pinget 2016).

The ARD solutions that migrated southwards to the Calama basin along the Exótica valley moved mainly as surficial run-off directly on the bedrock producing strong kaolinization and chrysocolla/copper wad impregnation of the Paleozoic metamorphic and granitic bedrock (Fig. 12A). This mineralization mainly in the bedrock is the first one to be recognized in the Exótica deposit. Manganese to form copper pitch/wad was available from dissolution of late-stage hypogene Mn-bearing carbonates in the Chuquicamata orebody (Ossandón et al. 2001; Pinget 2016). Presently, it is observed in the arid conditions of northern Chile that evaporation of very acid waters favors the formation of efflorescent salts and crusts of copper and iron sulfates and/or chlorides (Bandy 1938; Nordstrom and Alpers 1999; Dold 2006; Smuda et al. 2014), which can store free sulfuric acid (e.g., rhomboclase [$(H_3O)Fe(SO_4)_2 \cdot 3H_2O$]) (Nordstrom and Alpers 1999). Acidity is buffered by ferric iron hydroxides and hydroxide sulfates like goethite, jarosite, and schwertmannite ($Fe^{3+}{}_{16}O_{16}(SO_4)_2(OH)_{12} \bullet nH_2O$) at around pH 2–4 (Alarcon et al. 2014). When occasional

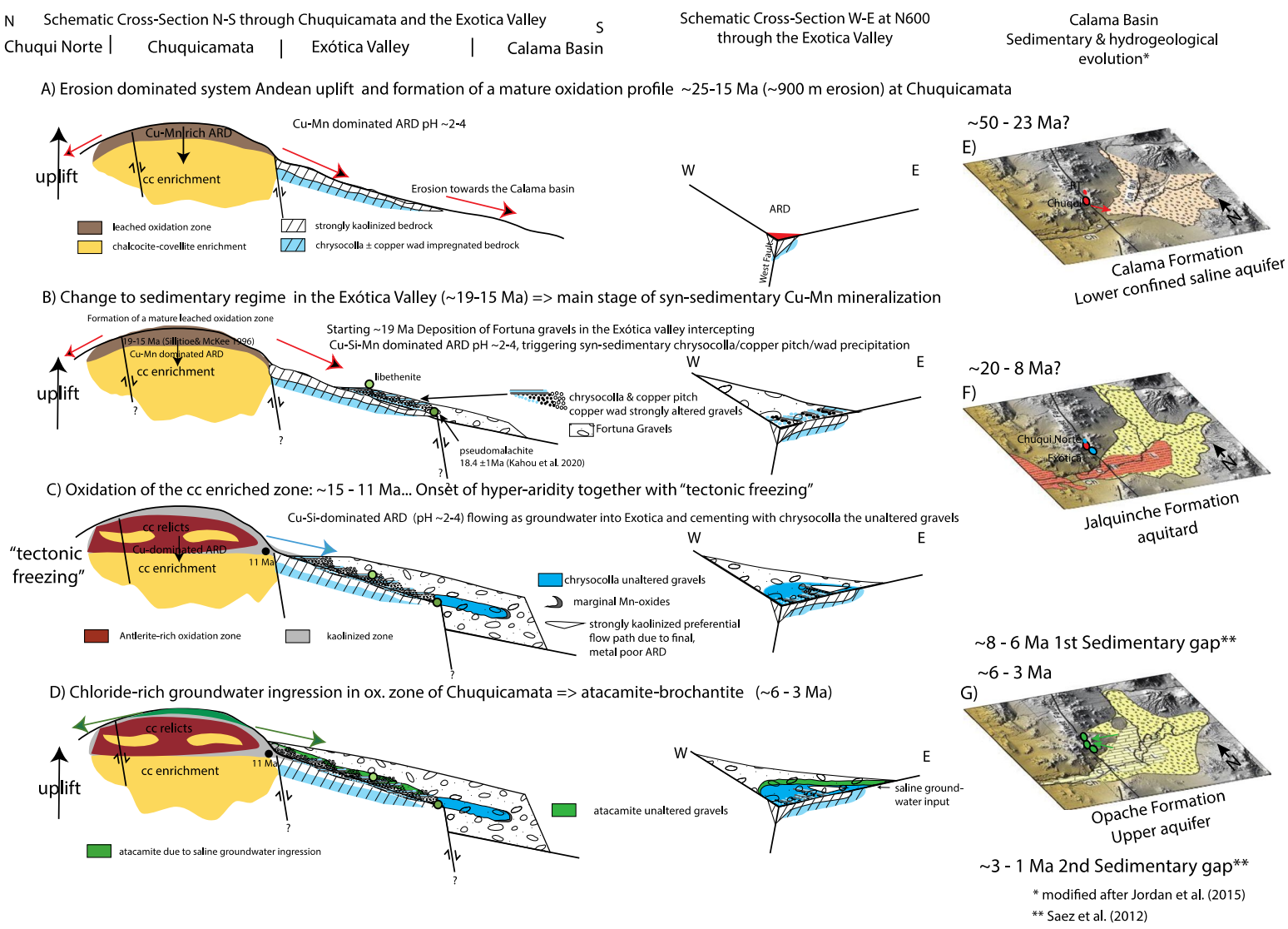

Fig. 12 Genetic model of the formation of the Exótica mineral assemblage in relation to the tectonic and climatic evolution of the Chuquicamata–Calama area. **A–D** represent the four mineralization steps and their respective mineral assemblages visualized in a N-S cross section through the Chuquicamata/Exótica Complex and in the center the corresponding W-E cross section (for location of the cross-sections see Fig. 1 I). **E–G** show the sedimentary and hydrogeological evolution of the Calama Basin after Jordan et al. (2015). The red dot in **E** represents the oxidizing Chuquicamata ore and the red arrow the ARD flow direction. **F** The light blue dots North and South of Chuquicamata represent the Chuqui Norte and Exótica chrysocolla/copper pitch wad mineralization, respectively. **G** The green dots show the atacamite distribution due to groundwater input (green arrows) into Chuquicamata and up to Radomiro Tomic in the north and the northern part of Exótica in the South. For discussion. see text

rainwater interacts with the soluble efflorescent salts and crusts, it is rapidly acidified and charged in ions. At Chuquicamata, these processes are thought to have been significant in Miocene times, and the so acidified sporadic rainwaters could react with chalcanthite and antlerite–brochantite, the main copper-bearing minerals of the oxidation zone of the Chuquicamata deposit (Bandy 1938; Pinget 2016), as well as with manganese oxides (e.g., birnessite). Geochemical equilibration of rainwater with the secondary minerals in the oxidation zone would result in highly oxidative (Eh > 1.0 V), acidic (pH ~ 1–3), and Cu-Mn-Si-dominated solutions (Pinget 2016). During its flow through the Chuquicamata Fe(III) hydroxide-rich oxidation zone, the solution would be buffered by the Fe(III) hydroxides to a pH of ~ 2–4 (Jurjovec et al. 2002, 2003), the pH we assume for the laterally percolating Cu-Mn-Si-dominated ARD solutions entering the Exótica valley.

B. ***Formation of the main chrysocolla–copper pitch/wad mineralization at Exótica ~19–15 Ma*** (Fig. ***12B***)

While in the Chuquicamata porphyry copper deposit exhumation and erosion and the formation of a mature supergene profile continued as documented by supergene alunite ages between 19 and 15 Ma (Sillitoe 2005), a change from a mainly erosive to a sedimentary regime was registered after 19 Ma in the Exótica valley, after the 35 km strike-slip displacement of the presently adjacent Fortuna granodiorite, with the beginning of the deposition of the Fortuna gravels (Lindsay 1998). This change caused that the Cu-Mn-Si-dominated ARD solutions from Chuquicamata were now intercepted by the Fortuna gravels. The gravels, mainly consisting of fresh Fortuna granodiorite clasts, favored neutralization reactions as reflected by widespread kaolinization. The resulting pH increase, possibly together with evaporation processes (Fernández-Mort et al. 2018), led to supersaturation and the extensive precipitation of chrysocolla/copper pitch/wad (Fig. 12B). The beginning of sedimentation of the Fortuna gravels at < 19 Ma, the main host of the Exótica mineralization, correlates well with the 18.4 ± 1 Ma U–Pb age obtained on pseudomalachite in chrysocolla by Kahou et al. (2021). The deposition of the Fortuna gravels in the Exótica valley lasted until ~ 8 Ma (dated on an ash-tuff horizon 10–30 m below surface, with a K/Ar age of 8.4 ± 0.4 Ma) (Mortimer et al. 1978).

Close to the source of the Chuquicamata Cu-Mn-Si-dominated ARD lateral outflow, the gravel thickness is smaller than in distal parts, and the flow is more surficial, so that close to the source, surficial run-off can be assumed, and surficial pond formation was possible. Therefore, massive interlayered chrysocolla/copper pitch is mainly found in the northern part of Exótica (Fig. 3C). With distance, the water infiltrated into the gravels and flowed at deeper levels, where thinner layers of copper wad dominate. Since, in comparison to surficial run-off, porewater has stronger water–rock interaction with the sediment clasts and is prone for capillary transport, the higher compositional variability of the solutions contributed to the observed compositional heterogeneity of copper wad.

Münchmeyer (1996) reports 200 m of total gravel thickness at the N400 section (i.e., at a relatively proximal position) (Fig. 2), of which 70 m is mineralized in the lower part. Assuming a constant gravel deposition rate between 19 and 8 Ma in the Exótica valley, about 4 Ma would have been needed to deposit the lower third of the Fortuna gravels. Actually, the deposition rate before the onset of the hyper-arid conditions at ~ 15 Ma was possibly higher, so that a time span shorter than 4 Ma is more likely. Taking in account mostly surficial run-off, and therefore mostly syn-sedimentary copper pitch/wad formation, it can be suggested that the Mn-rich mineralization was mainly formed between ~19 and 15 Ma. A 15 Ma age for the end of the main chrysocolla–copper pitch/wad mineralization episode correlates with the change to a reduced uplift rate because the Central Andes entered a tectonic and erosional "freezing" period (Armijo et al. 2015). This correlates well with the onset of hyper-aridity at around 15–14 Ma proposed by several authors (Jordan et al. 2014; Armijo et al. 2015) and with changes in the geochemistry of paleo-soils in the Calama basin reflecting the change from semi-arid to hyper-arid (200 to 20 mm/a of rainfall) conditions between 19 and 13 Ma (Rech et al. 2006).

C. ***Oxidation of the enriched chalcocite blanket at Chuquicamata and chrysocolla mineralization in unaltered gravels (~ 15–11 Ma) (Fig.*** 12C)

The above mentioned tectonic "freezing" and the change to hyper-arid conditions largely stopped in Chuquicamata the uplift-driven enrichment process at around 15 Ma and favored the drop of the groundwater level and of the limit of oxidation and leaching of the enriched chalcocite blanket down by about 300 m (Fig. 12C). The oxidation process lasted at least until 11 Ma, as indicated by a dated supergene alunite vein in the lower part of the oxidized zone in the southernmost part of the Chuquicamata open pit (K. Wemmer, written communication, 2018) but possibly was subsequently reactivated during sporadic wetter periods. The enriched chalcocite blanket was oxidized and leached out mainly in the quartz-sericitic alteration and chloritic alteration zones, whereas the antlerite ore remained in the potassic alteration zone. Taking in account the mineralogy of the chalcocite blanket, the drainage derived from its oxidation was strongly acidic (pH ~2–4), Cu-Si-dominated,

and had higher Cu and lower Mn concentrations than that derived from the mature first oxidation zone. With the progressive deposition of the Fortuna gravels, the system changed from superficial towards deeper flow, so that these solutions started to migrate as groundwater under increasingly reducing conditions, favoring chrysocolla precipitation that cemented mainly unaltered gravels.

As Mn(II) has high solubility in reducing conditions, a small amount of Mn from preexisting copper pitch/wad was probably dissolved along the underground flow path. This Mn was transported southwards to the margin of the exotic mineralization where it precipitated as the copper wad halo external to the zone of massive chrysocolla in unaltered gravels following the reaction scheme of Fig. 11. As described above, this zoning was still visible during sampling in the middle of the pit wall of the southern Exótica pit.

Taylor (1935) describes strong leaching below the antlerite orebody in the southern part of the supergene profile of Chuquicamata (Fig. 12). We interpret this to have happened in the last stages of oxidation activity at Chuquicamata, still under the tectonically freezing period proposed by Armijo et al. (2015). Because of the lack of uplift, eventually no more metal sulfides were available for oxidation, so that the system finally became leached out. Subsequently, the flow path caused by sporadic rainfalls would be acidified through interaction with mainly Fe(III) hydroxide/hydroxide sulfate assemblages, poor in Cu. The resulting solution would be therefore poor in Cu and relatively rich in Al and Si, i.e., a composition similar to that obtained in laboratory leach-out experiments with sulfide-bearing tailings and with mixtures with jarosite (Jurjovec et al. 2003).

This acidic, but metal-poor ARD fluid is seen as responsible for the final and main kaolinization of the host rock in the "channel" in the northern part of Exótica. There, the strongly kaolinized central alteration zone (Fig. 3A) is not seen to have been formed by migration of acid metal-rich solutions that subsequently built-up the cemented Cu-Mn mineralization, but it is interpreted as the retreat of acidic, but metal-poor solutions during the final episode of the drainage of the oxidation of the chalcocite enriched zone of the supergene profile of Chuquicamata. These acidic solutions overprinted and partly dissolved the preexisting chrysocolla/copper pitch mineralization and locally re-precipitated it in secondary chrysocolla veinlets, as visible in Fig. 3C.

D. ***Chloride-rich groundwater ingression: atacamite/brochantite mineralization (~6–3 Ma)*** (Fig. 12D)

The presence of atacamite in the oxidation zone of the Chuquicamata deposit is only reported in the upper 30 m below surface (Bandy 1938; Jarrell 1944; Pinget 2016). This contrasts with the situation at the topographically lower Radomiro Tomic deposit, where the whole oxidation zone (about 300 m thick) is mineralized with atacamite (Cuadra and Rojas 2001). In Exótica, atacamite–brochantite (Figs. 2, 4, and 12D) occur mainly cementing cracks and pore spaces in unaltered gravels in the uppermost part of the mineralization in the northern part of the deposit (Münchmeyer 1996). Atacamite–brochantite cross-cuts all previous mineral assemblages, constituting the latest Cu deposition stage of Exótica, followed only by gypsum veinlets that cross-cut also atacamite. The $\delta^{34}S$ ratios around −2 ‰ from a brochantite–atacamite vein from Exótica suggests that the sulfur derives from sulfide oxidation at Chuquicamata (Lambiel et al. 2022).

In the sampling campaign in 2009, pure atacamite precipitation was observed in the southeastern end of the Exótica pit at an outflow of a saline aquifer of the Calama basin (sample EX2: pH 5.67; Cl = 17 g/L, Cu = 239 mg/L) (Lambiel 2013; Lambiel et al. 2022). Geochemical modeling on sample EX2 suggests that Cu(I) transported in the saline aquifer is stable as $CuCl_2^-$ complex below Eh = 0.5 V. In contrast, when it outflows to more oxic conditions (> 0.5 V), it oxidizes to Cu(II) and forms $CuCl^+$ complexes, which subsequently hydrolyze to atacamite, resulting in acidification to a pH of 5.67 in the case of sample EX2 (Lambiel et al. 2022). Therefore, the formation of atacamite suggests oxic (Eh > 0.5 V) conditions and high Cl concentration as well as pH higher than ~5.5.

The $\delta^{37}Cl$ signatures of atacamite from the oxidation zone in Radomiro Tomic, Chuquicamata, and Exótica indicate the same chloride source (Arcuri and Brimhall 2003), pointing to a related mineralization event in all three deposits. The confined lower saline aquifer in the Calama basin (Dirección General de Aguas 2003; Smuda et al. 2014) offers a plausible Cl source for the formation of atacamite.

How the Cl-rich groundwater from the lower saline aquifer could have entered into the topographically highest parts of the Radomiro Tomic–Chuquicamata–Exótica complex to form atacamite is disscussed here. Today, chloride and fluoride-rich and sulfate-poor groundwater with a pH of 6.6–7.3 and a hydraulic gradient from South to North is reported by Cuadra and Rojas (2001) in topographically lower areas of Radomiro Tomic (RT), around 3 km N of Chuquicamata. Jordan et al. (2015) describe the current hydrogeological conditions of the Calama basin and show that the lower aquifer (2550 m) is topographically lower than the upper part of the Chuquicamata and Exótica deposits in which atacamite is observed (2900–3000 m). The most logical explanation to overcome this 400-m-altitude difference

is based on a combination of tectonic processes and a wetter period with higher groundwater levels than those observed today. The tectonic uplift of > 900 m in the last 10 Ma caused by divergent orogenic growth due to subduction of the Brazilian shield below the Andes (Rech et al. 2006; Armijo et al. 2015) is probably part of the explanation as already proposed by Cameron et al. (2007). The sedimentary record in the Calama basin suggests that the conditions for a connection of the confined lower saline aquifer of the Calama basin with the upper oxidation zone of Chuquicamata were last given between 6 and 3 Ma, when the palustrine-lacustrine limestones of the Opache Formation formed in the western margin of the Calama basin (May et al. 2005). Also, the breakthrough of the closed Calama basin by the Loa river after 3 Ma (May et al. 2005), resulting in drainage towards the Quillagua-Tamarugal basin and finally into the Pacific (Sáez et al. 2012), caused a decrease of the groundwater levels in the Calama basin towards the presently observed levels.

Therefore, we suggest that, most likely between 6 and 3 Ma, hydraulic connections of the saline lower aquifer of the Calama basin and the upper part of the RT–Chuquicamata–Exótica complex, allowed the ingression of neutral, Cl-rich groundwater in the upper oxidation zone of Chuquicamata–RT (Fig. 12D). At the local scale, the ingression was artesian and produced seepage at the NE and NNW fault systems described by Skarmeta (2020) in the northeast and southeast parts of Chuquicamata. That the hydraulic regime was partly artesian is supported by the present situation in the Calama basin where Jordan et al. (2015) propose local discharges of the lower into the upper aquifer, specifically in the western part of the Calama basin in vicinity of the RT–Chuquicamata–Exótica complex.

The saline outflow resulted in the dissolution of existing soluble copper sulfates like chalcanthite present in the oxidation zone. Where the neutralization potential was able to maintain the pH above ~5.5, atacamite could form in situ. However, an important amount of copper was mobilized in slightly acidic Cu-Ca–Cl-SO_4 solution following the hydraulic gradient to the south, towards Exótica, and to the north, towards RT, forming also atacamite–brochantite–gypsum assemblages on top of the preexisting mineralization of chrysocolla/copper pitch/wad, as well as pore space filling in unaltered gravels.

The main formation of atacamite in the period between 6 and 3 Ma is not consistent with the ~ 240 ka age proposed by Reich et al. (2009) based on U-Th dating of gypsum intergrown with atacamite in a vein of the Chuquicamata pit. Our SXRD experiment (Figs. 9 and 10) shows that gypsum may suffer dissolution–reprecipitation during each rainy event, while atacamite most probably can survive these sporadic events, as it is a hydroxide chloride with lower solubility than gypsum. This is consistent with the fact that several generations of gypsum are observed, including one contemporaneous with atacamite and gypsum veinlets that are post atacamite (Fig. 4). Therefore, the possibility that the gypsum dated by Reich et al. (2009) postdates the main stage of atacamite cannot be discarded nor that recent minor atacamite precipitation was possible as also shown by Lambiel et al. (2022) in neoformed gel-like deposits in the southern end of the Exótica pit.

Conclusions

This study provides new data to understand the nature and conditions of formation of copper pitch, copper wad, and chrysocolla in the Exótica deposit downstream of the Chuquicamata porphyry copper deposit. The application of detailed mineralogical and textural studies combined with sequential X-ray diffraction (SXRD) and geochemical modeling helped to solve the "copper pitch/wad" enigma. Copper pitch and copper wad are essentially chrysocolla with co-precipitated Mn oxides, mainly birnessite, as well as pseudo-amorphous Mn oxide/oxyhydroxides. Copper pitch formed at Exótica most likely in a low flow superficial regime, e.g., in ponds or slopes, mainly close the source of ARD in the northern part of the deposit, while copper wad formed as thin patinas on rock and mineral surfaces. In the second case, increased direct water–rock interaction triggered higher compositional heterogeneity. Geochemical modeling suggests that birnessite (i.e., constituent together with chrysocolla of copper pitch/wad) formed in an acidic and highly oxidizing environment (typical of surficial run-off), in which the acidic mineralizing solutions altered the hosting gravels. In contrast, pure chrysocolla cementing mainly unaltered gravels formed in a more reducing and less acidic environment (typical for groundwater flow). Atacamite is the latest and minor, mineralization event cross-cutting all previous copper-bearing mineral assemblages.

Changes in tectonic and climatic conditions in the Chuquicamata area suggest the following mineralization sequence in four steps (Fig. 12), which can explain the textural relationships and mineral associations observed in Exótica from the geochemical point of view:

In step 1, Cu-Mn-Si-dominated acid (pH ~ 2–4) solutions from the Chuquicamata supergene oxidation profile percolated downstream on the bedrock of the Exótica valley (~ 30–25 to 19 Ma), resulting in the strongly kaolinized and chrysocolla/copper wad-impregnated bedrock as a result of pH increase through water–rock interaction.

These solutions were since ~ 19 Ma intercepted by gravels with the beginning of the deposition of the Fortuna gravels, triggering the syn-sedimentary formation of massive chrysocolla/copper pitch ore in the north and copper wad more to the south. In addition to pH increase through water–rock interaction, precipitation was favored by evaporation in ponds (step 2).

Erosion during a period of tectonic freezing and onset of hyper-aridity around 15 Ma exposed the supergene chalcocite blanket at Chuquicamata to oxidation down to 300 m, resulting in an acidic (~ pH 2–4), Cu-Si-dominated solution, with less Mn than the previous ARD event, that percolated as groundwater into the Exótica valley, cementing unaltered gravels with chrysocolla (step 3). At the end of the oxidation process of the chalcocite blanket, the solutions percolating through the Fortuna gravels were still acidic but copper-poor, resulting in strong kaolinization of the gravels and forming the central strongly kaolinized zone in the northern part of Exótica. In step 4, saline groundwater ingression (~6–3 Ma) in the upper part of the Chuquicamata oxidation zone triggered the dissolution of copper sulfate minerals present in the oxidation zone of Chuquicamata and the percolation of Cu-Cl-SO_4-dominated solutions (pH 5–7) in pore spaces on the mineralized chrysocolla–copper pitch/wad and kaolinized gravels in Exótica. As a result, atacamite/brochantite precipitated with gypsum in pore and crack fillings where high enough pH (> 5.5) and redox (> 0.5 V) were encountered and the permeability allowed the impregnation by mineralizing solutions. Gypsum veinlets represent the latest event in Exótica, cross-cutting all previous mineralization.

Supplementary Information The online version contains supplementary material available at https://doi.org/10.1007/s00126-022-01147-7.

Acknowledgements We thank the management and the geological team of CODELCO Norte (Chuquicamata mine and Mina Sur) for their permission, support, and constructive collaboration to make this work possible; we specially thank Manuel Vergara, Fernando Ramirez, Victorino Moyano, José (Pepe) Rojas, and their collaborators, and specially Carlos Barrios, for their inestimable help. We also thank, at the University of Geneva, A. Martigner for SEM analysis, J. Poté for ICP analysis, D. Ariztegui, S. Castelltort, and R. Cerny for their helpful advice, F. Capponi for XRF analysis and J.-M. Boccard and Frederic Arlaud for technical support, and Prof. Brian Townley (University of Chile, Santiago de Chile) for his review and English corrections. Prof. Gregor Borg and two anonymous reviewers are acknowledged for their helpful suggestions and corrections to improve this manuscript.

Funding Research financed by the Swiss National Science Foundation, Projects FNS 200021_129988 and 146484. Open access funding provided by University of Geneva

Declarations

Competing interests The authors declare no competing interests.

References

Ague JJ, Brimhall G (1989) Geochemical modeling of steady state fluid flow and chemical reaction during supergene enrichment of porphyry copper deposits. Econ Geol 84:506–528

Alarcon R, Gaviria J, Dold B (2014) Liberation of adsorbed and co-precipitated arsenic from jarosite, schwertmannite, ferrihydrite, and goethite in seawater. Minerals 4:603–620

Alpers CN, Brimhall GH (1989) Paleohydrologic evolution and geochemical dynamics of cumulative supergene metal enrichment at La Escondida, Atacama Desert, northern Chile. Econ Geol 84:229–255

Anderson JA (1982) Characteristics of leached capping and techniques of appraisal. In: Titley SR (ed) Advances in geology of the porphyry copper deposits, southern North America. University Arisona Press, Tucson, pp 275–295

Arcuri T, Brimhall GH (2003) The chloride source for atacamite mineralization at the Radomiro Tomic porphyry copper deposit, Northern Chile. Econ Geol 98:1667–1681

Armijo R, Lacassin R, Coudurier-Curveur A, Carrizo D (2015) Coupled tectonic evolution of Andean orogeny and global climate. Earth Sci Rev 143:1–35

Bandy MC (1938) Mineralogy of three sulphate deposits of Northern Chile. Am Miner 23:669–760

Billiet V (1942) The relations of chrysocolla, katangite, plancheite, bisbeeite, shattuckite and dioptase. Verh Kon Vlaamsche Acad Wetensch, Letteren Schoone Kunsten Belgie, Klasse Wetensch 4:58

Braxton D, Mathur R (2011) Exploration applications of copper isotopes in the supergene environment: a case study of the Bayugo porphyry copper-gold deposit, southern Philippines. Econ Geol 106:1447–1463

Brimhall GH, Alpers CN, Cunningham AB (1985) Analysis of supergene ore-forming processes and groung-water solute transport using mass balance principles. Econ Geol 80:1227–1257

Caley ER, Richards JFC (1956) Teophrastus on stones. Ohio State University, Columbus Ohio, pp 238

Cameron EM, Leybourne MI, Palacios C (2007) Atacamite in the oxide zone of copper deposits in northern Chile: involvement of deep formation waters? Miner Deposita 42:205–218

Campos E, Menzies A, Sola S, Hernández V, Riquelme R (2015) Understanding exotic-Cu mineralisation: part I - characterization of chrysocolla. Proceedings 13th SGA meeting. Nancy, pp 1153–1155

Chukhrov FV, Zvyagin BB, Gorshkov AI, Ermilova LP, Rundnitskaya ES (1968) About chrysocolla. Doklady Akademii Nauk SSSR Earth Sci Sect 6:29–44

Cooper FJ, Adams BA, Blundy JD, Farley KA, McKeon RE, Ruggiero A (2016) Aridity-induced Miocene canyon incision in the Central Andes. Geology 44:675–678. https://doi.org/10.1130/g38254.1

Crane MJ, Sharpe JL, Williams PA (2001) Formation of chrysocolla and secondary copper phosphates in the highly weathered supergene zones of some Australian deposits. Rec Aust Mus 53:49–56

Cuadra PC, Rojas GS (2001) Oxide mineralization at the Radomiro Tomic porphyry copper deposit, northern Chile. Econ Geol 96:387–400

Dirección General de Aguas (2003) Determinación de los derechos de aprovechamiento de agua subterránea factibles de constituir en los sectores de Calama y llalqui, Cuenca del Rio Loa, II Region, Chile. Gobierno de Chile. Ministerio de Obras Publicas. Dirección General de Aguas. Departament de Administración de Recursos Hidricos, Santiago de Chile.

Dold B (2003a) Dissolution kinetics of schwertmannite and ferrihydrite in oxidized mine samples and their detection by differential X-ray diffraction (DXRD). Appl Geochem 18:1531–1540

Dold B (2003b) Speciation of the most soluble phases in a sequential extraction procedure adapted for geochemical studies of copper sulfide mine waste. J Geochem Explor 80:55–68

Dold B (2006) Element flows associated with marine shore mine tailings deposits. Environ Sci Technol 40:752–758

Evenstar LA, Mather AE, Hartley AJ, Stuart FM, Sparks RSJ, Cooper FJ (2017) Geomorphology on geologic timescales: evolution of the late Cenozoic Pacific paleosurface in Northern Chile and Southern Peru. Earth Sci Rev 171:1–27

Farges F, Benzerara K, Brown JGE (2006) Chrysocolla redefined as spertiniite In: SLAC-PUB-12232 (ed) 13th International Conference on X-ray absorption fine structure (XAFS13). Stanford, California, p 4

Fernández-Mort A, Riquelme R, Alonso-Zarza AM, Campos E, Bissig T, Mpodozis C, Carretier S, Herrera C, Tapia M, Pizarro H, Muñoz S (2018) A genetic model based on evapoconcentration for sediment-hosted exotic-Cu mineralization in arid environments: the case of the El Tesoro Central copper deposit, Atacama Desert, Chile. Miner Deposita 53:775–795

Fleischer M (1969) New mineral names. Am Miner 54:990–994

Foote HW, Bradley WM (1913) On solid solution in minerals. IV. The composition of amorphous minerals as illustrated by chrysocolla. Am J Sci 36:180–184

Frost RL, Xi Y (2013) Is chrysocolla (Cu, Al)$_2$H$_2$Si$_2$O$_5$(OH)$_4$·nH$_2$O related to spertiniite Cu(OH)$_2$? - A vibrational spectroscopic study. Vib Spectrosc 64:33–38

Frost RL, Xi Y, Wood BJ (2012) Thermogravimetric analysis, PXRD, EDX and XPS study of chrysocolla (Cu, Al)$_2$H$_2$Si$_2$O$_5$(OH)$_4$·nH$_2$O - structural implications. Thermochim Acta 545:157–162

Guild FN (1929) Copper pitch ore. Am Miner 14:313–318

Hariu T, Arima H, Sugiyama K (2013) The structure of hydrated copper-silicate gels, an analogue compound for natural chrysocolla. J Mineral Petrol Sci 108:111–115. https://doi.org/10.2465/jmps.121022c

Hartley AJ, Rice CM (2005) Controls on supergene enrichment of porphyry copper deposits in the Central Andes: a review and discussion. Miner Deposita 40:515–525

Jarrell OW (1944) Oxidation at Chuquicamata, Chile. Econ Geol 39:251–286

Jordan TE, Kirk-Lawlor NE, Blanco NP, Rech JA, Cosentino NJ (2014) Landscape modification in response to repeated onset of hyperarid paleoclimate states since 14 Ma, Atacama Desert, Chile. GSA Bull 126:1016–1046

Jordan T, Lameli CH, Kirk-Lawlor N, Godfrey L (2015) Architecture of the aquifers of the Calama Basin, Loa catchment basin, northern Chile. Geosphere 11:1438–1474

Jurjovec J, Ptacek CJ, Blowes DW (2002) Acid neutralization mechanisms and metal release in mine tailings: a laboratory column experiment. Geochim Cosmochim Acta 66:1511–1523

Jurjovec J, Ptacek CJ, Blowes DW, Jambor JL (2003) The effect of natrojarosite addition to mine tailings. Environ Sci Technol 37:158–164

Kahou ZS, Brichau S, Poujol M, Duchêne S, Campos E, Leisen M, d'Abzac F-X, Riquelme R, Carretier S (2021) First U-Pb LA-ICP-MS in situ dating of supergene copper mineralization: case study in the Chuquicamata mining district, Atacama Desert, Chile. Miner Deposita 56:239–252

Lambiel F (2013) New insights into the ore genesis of the Exotica deposit at Chuquicamata (Northern Chile) through the neoformation of Cu-oxide minerals from gel-like precursors. Institute of Earth Sciences. University of Geneva, MSc thesis, p 96

Lambiel F, Dold B, Spangenberg J, Fontboté F (2022) Neoformation of exotic copper minerals from gel-like precursors at the Exótica deposit, Chuquicamata, Chile. Miner Deposita. https://doi.org/10.1007/s00126-022-01148-6

Lindsay DD (1998) Structural control and anisotropy of mineralization in the Chuquicamata porphyry deposit, Chile. Dalhousie University, Halifax, NS, PhD thesis, p 381

Lynne BY, Campbell KA, Moore JN, Brown PRL (2005) Diagenesis of a 1900-year-old siliceous sinter (opal-A to quartz) at Opal Mound, Roosevelt Hot Springs, Utah, U.S.A. Sed Geol 179:249–278

Majzlan J (2020) Processes of metastable-mineral formation in oxidation zones and mine waste. Mineral Mag 84:367–375

Majzlan J, Navrotsky A, McCleskey RB, Alpers CN (2006) Thermodynamic properties and crystal structure refinement of ferricopiapite, coquimbite, rhomboclase, and Fe$_2$(SO$_4$)$_3$(H$_2$O)$_5$. Eur J Mineral 18:175–186

Majzlan J, Zittlau AH, Grevel K-D, Schliesser J, Woodfield BF, Dachs E, Števko M, Chovan M, Plášil J, Sejkora J, Milovská S (2015) Thermodynamic properties and phase equilibria of the secondary copper minerals libethenite, olivenite, pseudomalachite, kröhnkite, cyanochroite, and devilline. Can Mineral 53:937–960

May G, Hartley AJ, Stuart FM, Chong G (1999) Tectonic signatures in arid continental basins: an example from the Upper Miocene-Pleistocene, Calama Basin, Andean forearc, northern Chile. Palaeogeogr Palaeoclimatol Palaeoecol 151:55–77

May G, Hartley AJ, Chong G, Stuart F, Turner P, Kape SJ (2005) Eocene to Pleistocene lithostratigraphy, chronostratigraphy and tectono-sedimentary evolution of the Calama Basin, northern Chile. Rev Geol Chile 32:33–58

Menzies A, Campos E, Hernández V, Sola S, Riquelme R (2015) Understanding exotic-Cu mineralisation: part II - characterisation of black copper (cobre negro) ore. Proceedings volume, 13th SGA meeting, Nancy 1177–1180

Moreton S (2007) Copper-bearing silica gel from the walls of Tankardstown Mine, Co., Waterford. Ireland J Russell Soc 10:10–17

Mortimer BC, Münchmeyer FC, Urqueta DI (1978) Emplazamiento del yacimiento Exótica, Chile. Revista Geológica De Chile 6:41–51

Mote TI, Becker TA, Renne P, Brimhall GH (2001) Chronology of exotic mineralization at El Salvador, Chile, by Ar-40/Ar-39 dating of copper wad and supergene alunite. Econ Geol 96:351–366

Münchmeyer C (1996) Exotic deposits-products of lateral migration of supergene solutions from porphyry copper deposits In: Camus F, Sillitoe RH, Petersen R (eds) Andean copper deposits: new discoveries, mineralization, styles and metallogeny. Soc Econ Geol Special Publ 5:43–58.

Newberg DW (1967) Geochemical implications of chrysocolla-bearing alluvial gravels. Econ Geol 62:932–956
Nicolau C, Reich M, Lynne B (2014) Physico-chemical and environmental controls on siliceous sinter formation at the high-altitude El Tatio geothermal field, Chile. J Volcanol Geoth Res 282:60–76
Nordstrom DK, Alpers CN (1999) Geochemistry of acid mine waste In: Plumlee GS, Logsdon MJ (eds) The environmental geochemistry of ore deposits part A: processes, techniques, and health issues. Reviews in Economic Geology, vol 6A. Littleton, Colorado, pp 133–160
Oosterwyck-Gastuche MC (1970) La structure de la chrysocolle. Comptes Rendus De L'académie Des Sciences De Paris 271:1837–1840
Ossandón G, Fréraut R, Gustafson LB, Lindsay D, Zentilli M (2001) Geology of the Chuquicamata mine: a progress report. Econ Geol 96:249–270
Padilla Garza RA, Titley SR, Pimentel BF (2001) Geology of the Escondida porphyry copper deposit, Antofagasta Region, Chile. Econ Geol 96:307–324. https://doi.org/10.2113/gsecongeo.96.2.307
Parkhurst DL, Appelo CAJ (2013) Description of input and examples for PHREEQC version 3—a computer program for speciation, batch-reaction, one-dimensional transport, and inverse geochemical calculations. U.S. Geological Survey Techniques and Methods, Denver Colorado, Book 6, chap. A43, p 497
Perelló J, Cox D, Garamjav D, Sanjdorj S, Diakov S, Schissel D, Munkhbat T-O, Oyun G (2001) Oyu Tolgoi, Mongolia: Siluro-Devonian porphyry Cu-Au-(Mo) and high-sulfidation Cu mineralization with a Cretaceous chalcocite blanket. Econ Geol 96:1407–1428
Perelló J, Razique A, Schloderer J, Asad-ur-Rehman (2008) The Chagai porphyry copper Belt, Baluchistan Province, Pakistan. Econ Geol 103:1583–1612
Pincheira M, Dagnino A, Kelm U, Helle S (2003) Copper pitch y copper wad. Contraste entre las fases presentes en las cabezas y en los ripios en pruebas de lixiviación de materiales de Mina Sur, Chuquicamata. 10º Congreso Geológico Chileno. Concepción, pp 10
Pinget M-C (2016) Supergene enrichment and exotic mineralization at Chuquicamata, Chile. University of Geneva, Geneva, PhD thesis, pp 182
Pinget M-C, Dold B, Zentilli M, Fontboté L (2015) Reported supergene sphalerite rims at the Chuquicamata porphyry deposit (Northern Chile) revisited: Evidence for a hypogene origin: Econ Geol 110:253–262
Prosser AP, Wright AJ, Stephens JD (1965) Physical and chemical properties of natural copper silicates which resemble chrysocolla. Trans Ins Min Metall B 74:233–258
Rech JA, Currie BS, Michalski G, Cowan AM (2006) Neogene climate change and uplift in the Atacama Desert, Chile. Geology 34:761–764
Reich M, Palacios C, Vargas G, Luo SD, Cameron EM, Leybourne MI, Parada MA, Zuniga A, You CF (2009) Supergene enrichment of copper deposits since the onset of modern hyperaridity in the Atacama Desert, Chile. Miner Deposita 44:497–504
Riquelme R, Tapia M, Campos E, Mpodozis C, Carretier S, González R, Muñoz S, Fernández-Mort A, Sanchez C, Marquardt C (2018) Supergene and exotic Cu mineralization occur during periods of landscape stability in the Centinela Mining District, Atacama Desert. Basin Res 30:395–425
Sáez A, Cabrera L, Garcés M, Pvd B, Jensen A, Gimeno D (2012) The stratigraphic record of changing hyperaridity in the Atacama desert over the last 10 Ma. Earth Planet Sci Lett 355–356:32–38
Sanchez C, Brichau S, Riquelme R, Carretier S, Bissig T, Lopez C, Mpodozis C, Campos E, Regard V, Hérail G, Marquardt C (2018) Exhumation history and timing of supergene copper mineralisation in an arid climate: new thermochronological data from the Centinela District, Atacama, Chile. Terra Nova 30:78–85
Schwartz GM (1934) Paragenesis of the oxidized ores of copper. Econ Geol 29:55–75
Sillitoe RH, Mortimer C, Clark AH (1968) A chronology of landform evolution and supergene mineral alteration, southern Atacama Desert, Chile. Trans Inst Min Metall B 77:166–169
Sillitoe RH (2005) Supergene oxidized and enriched porphyry copper and related deposits. Economic Geology 100th Anniversary Volume, Society of Economic Geologists, Littleton, Colorado, pp 723–768
Skarmeta J (2020) Structural controls on alteration stages at the Chuquicamata copper-molybdenum deposit, northern Chile. Econ Geol 116:1–28
Smuda J, Dold B, Spangenberg JE, Friese K, Kobek MR, Bustos CA, Pfeifer H-R (2014) Element cycling during the transition from alkaline to acidic environment in an active porphyry copper tailings impoundment, Chuquicamata, Chile. J Geochem Explor 140:23–40
Sun M-S (1963) The nature of chrysocolla from Inspiration Mine, Arizona. Am Miner 48:649–658
Taylor AV (1935) Ore deposits of Chuquicamata, Chile. XVI Int Geol Congress, Washington, pp 473–484
Throop AH, Buseck PR (1971) Nature and origin of black chrysocolla in the Inspiration Mine, Arizona. Econ Geol 66:1168–1175
Vieillard P (2000) A new method for the prediction of Gibbs free energy of formation of hydrated clay minerals based on the electronegativity scale. Clays Clay Miner 48:459–473
Yu Q, Sasaki K, Tanaka K, Ohnuki T, Hirajima T (2012) Structural factors of biogenic birnessite produced by fungus Paraconiothyrium sp. WL-2 strain affecting sorption of Co^{2+}. Chem Geol 310–311:106–113